

CAPITAL UNIVERSITY OF SCIENCE AND
TECHNOLOGY, ISLAMABAD



Revisiting Backward Facing Step Problem with
Micromagnetorotation

by

Noor ul ain Azam

A thesis submitted in partial fulfillment for the
degree of Master of Philosophy

in the

Faculty of Computing
Department of Mathematics

2025

Copyright © 2025 by Noor ul ain Azam

All rights reserved. No part of this thesis may be reproduced, distributed, or transmitted in any form or by any means, including photocopying, recording, or other electronic or mechanical methods, by any information storage and retrieval system without the prior written permission of the author.

With heartfelt gratitude, I dedicate this thesis to my beloved parents, Muhammad Azam and Tahira Parveen, whose unwavering love and sacrifices have shaped my path; to my inspiring teacher Dr Muhammad sabeel khan, whose guidance and wisdom enlightened my journey; and to my supportive husband Junaid Ali, whose constant encouragement and patience have been my pillar of strength. I am deeply thankful to each of you for your profound impact on my life and success.



CERTIFICATE OF APPROVAL

Revisiting Backward Facing Step Problem with Micromagnetorotation

by

Noor ul ain Azam

(MMT213022)

THESIS EXAMINING COMMITTEE

S. No.	Examiner	Name	Organization
(a)	External Examiner	Dr. Aamir Ali	CUI, Attock Campus
(b)	Internal Examiner	Dr. Samina Batul	CUST, Islamabad
(c)	Supervisor	Dr. Muhammad Sabeel Khan	CUST, Islamabad

Dr. Muhammad Sabeel Khan
Thesis Supervisor
May, 2025

Dr. Muhammad Sagheer
Head
Dept. of Mathematics
May, 2025

Dr. Muhammad Abdul Qadir
Dean
Faculty of Computing
May, 2025

Author's Declaration

I, **Noor ul ain Azam** hereby state that my MPhil thesis titled “**Revisiting Backward Facing Step Problem with Micromagnetorotation**” is my own work and has not been submitted previously by me for taking any degree from Capital University of Science and Technology, Islamabad or anywhere else in the country/abroad.

At any time if my statement is found to be incorrect even after my graduation, the University has the right to withdraw my MPhil Degree.



(Noor ul ain Azam)

Registration No: MMT213022

Plagiarism Undertaking

I solemnly declare that research work presented in this thesis titled “**Revisiting Backward Facing Step Problem with Micromagnetorotation**” is solely my research work with no significant contribution from any other person. Small contribution/help wherever taken has been duly acknowledged and that complete thesis has been written by me.

I understand the zero tolerance policy of the HEC and Capital University of Science and Technology towards plagiarism. Therefore, I as an author of the above titled thesis declare that no portion of my thesis has been plagiarized and any material used as reference is properly referred/cited.

I undertake that if I am found guilty of any formal plagiarism in the above titled thesis even after award of MPhil Degree, the University reserves the right to withdraw/revoke my MPhil degree and that HEC and the University have the right to publish my name on the HEC/University website on which names of students are placed who submitted plagiarized work.



(Noor ul ain Azam)

Registration No: MMT213022

Acknowledgement

All the praise and appreciation are for almighty ALLAH who is the most beneficent and the most merciful created the universe and blessed the mankind with Intelligence and wisdom to explore His secrets. Countless respect and endurance for Prophet Muhammad (Peace Be Upon Him), the fortune of knowledge, who took the humanity out of ignorance and shows the right path.

I would like to show my gratitude and immeasurable respect to my supervisor Dr. Muhammad Sabeel Khan, Associate Professor, Capital University of Science and Technology, Islamabad who suggested the problem, extended all facilities and provided inspiring guidance for the successful completion of my research work. I deem it as my privilege to work under his able guidance.

Special thanks to my teacher Dr. Muhammad Sagheer, Professor, Capital University of Science and Technology, Islamabad for his kind, friendly, encouraging and enthusiastic attitude which gave me courage of facing ups and downs of the process. I have enjoyed every moment of insightful discussion with him, also thanks to Dr. Rashid Ali, Professor, Capital University of Science and Technology, Islamabad.

At this juncture, I pay my deep regards to my beloved parents and specially my brothers Mr. Farooq Azam, Mr. Shams ul Islam and Mr. usama waheed for their selfless care, love, devotion and prayers that made me able to achieve this goal. May Allah bless them all.

(Noor ul ain Azam)

Registration No: MMT213022

Abstract

In this thesis, a backward facing step problem in fluid mechanics is revisited. For this purpose, first the Navier-Stokes problem in two dimensions is simulated on a backward facing step flow geometry and numerical solutions are obtained for velocity fields. The Navier-Stokes equations are then coupled with the micropolar equation to extend the model in the micropolar flow. Further, the effect of micromagnetorotation (MMR) is considered and incorporated in the extended mathematical model. The extended model is described in the form of coupled system of partial differential equations (PDEs). Suitable boundary conditions on the backward facing step geometry is prescribed. The governing flow PDEs together with the associated boundary conditions describe the complete problem to solve. In order to solve the presented mathematical model problem finite element numerical procedure is adopted. In order to find the solution of the problem first the governing flow dynamic equations are non-dimensionalized together with the associated boundary conditions. The non-dimensionalized PDEs are then used to calculate the weak formulation of the problem. The calculated weak formulation afterwards is used to implement in the open source code FreeFEM++. The implemented code is first tested for accuracy and a comparison of computed re-attachment lengths with the implemented code is compared with the solution available in the literature. Results are obtained and discussed in the presence of MMR effect.

Contents

Author's Declaration	iv
Plagiarism Undertaking	v
Acknowledgement	vi
Abstract	vii
List of Figures	x
List of Tables	xi
Abbreviations	xii
Symbols	xiii
1 Introduction and Literature Review	1
1.1 Thesis Contribution	6
1.2 Thesis Attributes	6
2 Basic Terminologies and Finite Element Procedure	8
2.1 Introduction	8
2.2 Backward Facing Step Flow BFSF Problem	8
2.2.1 Geometrical Representation and Key Parameters	9
2.3 Types of Fluid Flow	10
2.3.1 Uniform Flow	10
2.3.2 Non-uniform Flow	10
2.3.3 Steady Flow	10
2.3.4 Unsteady Flow	11
2.3.5 Rotational Flow	11
2.3.6 Irrotational Flow	11
2.3.7 Laminar Flow	11
2.3.8 Turbulent Flow	12
2.3.9 Compressible Flow	12
2.3.10 Incompressible Flow	12
2.4 Fundamental Laws	12
2.4.1 The Continuity Equation	13

2.4.2	Conservation of Momentum	14
2.4.3	Conservation of Energy	15
2.5	Heat and Mass Transfer Phenomenon and Related Properties	16
2.5.1	Heat Transfer	16
2.5.2	Mass Transfer	16
2.5.3	Conduction	16
2.5.4	Convection	17
2.5.5	Natural Convection or Free Convections	17
2.5.6	Forced Convection	17
2.5.7	Radiation	17
2.6	Dimensionless Parametres	18
2.6.1	Reynolds Number	18
2.7	Finite Element Method	18
2.8	Galerkin Finite Element Method for Nonlinear PDEs	19
2.8.1	Weak Formulation	19
2.8.2	Galerkin Approximation	20
2.8.3	Discretization	20
2.8.4	Element Formulation and Assembly	20
2.9	Variational Formulation	21
2.10	2D Example: Heat Equation	22
2.11	Advantages of Galerkin FEM	23
2.12	Limitations of Galerkin FEM	23
3	Laminar Flow Over a Backward Facing Step	25
3.1	Introduction	25
3.2	Geometry of the Problem	26
3.3	Dimensional Form of the Governing Equations	26
3.4	Dimensional Boundary Conditions	27
3.4.1	Dimensionless Governing Equations with Boundary Condi- tions	28
3.5	Weak formulation of the Problem	31
3.6	Numerical Results and Discussion	32
4	Backward Facing Step Micropolar Flow with Micromagnetorota- tion	36
4.1	Introduction	36
4.2	Dimensional Governing Equations	36
4.2.1	Dimensionless Parameters	38
4.3	Conversion of Dimensional form into Dimensionless Form	38
4.4	Dimensionless Governing Equations	43
4.5	Weak formulation/Variational form of the problem	44
4.6	Results and Discussion	61
5	Conclusion and Future Work	65
	Bibliography	67

List of Figures

2.1	Backward facing step geometry	9
3.1	Backward facing step flow Configuration.	26
3.2	Velocity contours for varying Re . (a) For $Re = 50$ (b) For $Re = 150$ (c) For $Re = 500$	34
3.3	Velocity contours for varying channel's inlet height. (a) For $H = 1$ (b) For $H = 1.5$ (c) For $H = 2$	35
4.1	Velocity contours for varying Re with fine mesh. (a) For $Re = 50$ (b) For $Re = 150$ (c) For $Re = 500$	62
4.2	stream lines with and without MMR for different Reynolds number Re . (a) For $Re = 50$ without MMR (b) For $Re = 50$ with MMR (c) For $Re = 500$ without MMR (d) For $Re = 500$ with MMR	63

List of Tables

3.1	Reattachment length with varying Re	33
3.2	Maximum Stream function values with varying Re	33
4.1	Comparison of reattachment points with the literature.	61
4.2	Reattachment points with and without MMR effect.	61
4.3	Maximum Stream function values with and without MMR effect. . .	62

Abbreviations

BFS	Backward-Facing Step
BFSF	Backward-Facing Step Flow
CFD	Computational Fluid Dynamics
FEM	Finite Element Method
GWRM	Galerkin Weighted Residual Method
MFFS	Microscale Forward-Facing Step
MBFS	Microscale Backward-Facing Step
MMR	Micromagnetorotation
PDEs	Partial Differential Equations

Symbols

ρ	Density
μ	Dynamical viscosity
ξ_j	Shape function
η_j	Interpolation function
Re	Reynolds number
\tilde{w}	Weight function
K	Micropolar flow
Ω	Computational domain
\tilde{U}	Test function
\bar{W}	Infinite dimensional test space
γ^*	Spin gradient viscosity
E_r	Eringen number
K_m	Micro-inertial parameter
K^*	Block stiffness vector
X^*	Block solution vector
Q^*	Block boundary vector
u_i	Nodal variable
u	Dimensional x-component of velocity
v	Dimensional y-component of velocity
w	Dimensional microrotational velocity
U	Non-dimensional x-component of velocity
V	Non-dimensional y-component of velocity
W	Non-dimensional microrotational velocity

Chapter 1

Introduction and Literature Review

Early studies on this benchmark problem BFS flow began in the 1950s, focusing on understanding the behavior of fluid flow under various conditions. Flow separation became a significant area of research throughout the 20th century, with particular attention given to its occurrence in critical engineering applications such as the wings of airplanes, pipes, turbines, and the airflow around large structures like skyscrapers and tall buildings. These flows often experience sudden expansions, leading to complex flow patterns. Understanding the fluid dynamics in these regions has been crucial for optimizing designs in a variety of engineering fields. Studies on backward-facing steps and their associated flow features have provided valuable insights into turbulence, vortex behavior, and the influence of geometric variations on flow characteristics, making it an essential problem in fluid mechanics and a benchmark for experimental and computational investigations.

Geometry of the BFS is simple yet it exhibits complex flow behaviour. Flow separation is not the only feature, there are many other flow behaviours to study for practical purposes for example eddies, wakes, vortices, reverse flows, recirculation regions and reattachment of the flow etc. The horizontal distance between the step and the reattachment point is defined as the reattachment length [1]. The work has been investigated for this benchmark problem is both on laminar and turbulent models

Early works have been carried out using transformations with geometry and fundamental flow behaviour whereas advancement in numerical and computational areas was touched in 1980's [2]. The work on 2D configurations having horizontal, vertical and inclined backward-facing step was investigated by several researchers who reached at the conclusion that the effects of buoyancy forces on heat transfer is less in horizontal and more in vertical and inclined cases. Moreover, in case of the 2D horizontal backward-facing step with air circulation having uniform wall temperature revealed that Nu does not depend upon Re and with the increasing buoyancy force, recirculation region and Nu decreased [3]. Attributes of heat flow and mass transfer for BFS were studied by Iwai et al. [4] at low Re to explore the aspect ratio of the channel. Many heat exchanging device configurations, for example condensers, evaporators, boilers and BFS are similar in the sense that they have immediate expansions in their geometry. In 3D heat exchanging devices where all of the surrounding walls are heated, Nie and Armaly studied [5] 3D flow for wall temperature distributions, Nu and other important parameters in a BFS problem with rectangular duct. A helpful data for design optimization was obtained from this study. Armaly et al. inquired [6] experimentally and theoretically the flow over BFS using Laser Doppler measurements for velocity reattachment length, showing extra regions of flow separation which was not found in earlier literature.

Significance of nanofluids becomes higher when studied with backward-forward stepping. According to the work [7], the problem arises when reattachment and separation of fluid are encountered together. Effects of various parameters along with cylinder's angular velocity and volume fraction of the nanofluid were studied. Backward facing with nanofluids for heat transfer magnification with separated flows were studied by Abu-Nada in [8]. Aside from dissimilar nanofluid volume fraction, different types of nanoparticles were used as well. It was noticed that out of the recirculation zone, Nu was increased on using nanoparticles with high thermal ability and vice versa for those with low thermal ability, within the recirculation region. Steady mixed convective flow over 3D stepping is studied [9] by Saldana. A comparison between mixed and pure forced convection with differences between velocity and temperature distribution was numerically simulated.

Abu-Mulaweh provided a deep scrutiny on single-phase mixed convective flow [10] and transport of heat within the fluid in both forward and backward stepping at several unlike angles. Many of previously estimated inter depending variable quantities were reproduced by making some assumption and changing important parameters. Thermal behavior of nanofluids' with pulsating flow over BFS with a immobile cylinder was studied by Selimefendigil and Öztop [11]. Consequences of parameters like frequency, Re and ϕ on the flow and heat transfer features were investigated numerically. Enhanced oscillation frequency, Re and ϕ resulted in enhancement of heat transfer. Reduced order model is an attribute grounded on database of fluids and structural models. It helps in reduction of computational cost yet satisfactory precision. A revolving cylinder exposed to nanofluid over BFS with mixed convection was studied [7] for reduced order model. The impact of several parameters upon heat transfer was studied. An increment in heat transfer was seen on blend of specific parameters. Forced convection features with laminar flow over 2D backward stepping with circular cylinder was considered by Kumar and Dhiman [12].

Two dimensional laminar flow with mixed convection over a straight plane microscale backward stepping placed in channel was numerically inquired by Kherbeet et al. [13]. Several nanoparticles types were used to conduct the experiment. The Nu was noticed to be increased with increasing values of Re and nanofluid volume fraction which was highest with particles of Silicon dioxide (SiO_2). Again Kherbeet et al. [14] performed experiment for laminar nanofluids above microscale BFS to check the consequences upon heat transfer attributes. Heat transfer and fluid flow properties over a backward or forward stepping through duct with obstacles is worked upon by fewer researchers. A square obstacle positioned before the step in pulsating laminar flow above a backward stepping with varying Pr , Re and positions of obstacle were numerically investigated by Selimefendigil [15]. It was reported that obstacle position can be used as the key to handle heat transfer. Laminar nanofluids flow over backward stepping under forced convection was mathematically inquired [16]. The foot wall of the step was elastic. When Re and ϕ were increased, local and averaged heat transfer elevated. At highest Re , the heat transfer was highest with less elasticity of foot wall.

BFS or geometries with separated flow phenomena and reattachment come across several industrial, engineering and electronic devices. These include turbine blade cooling, combustion chamber cooling, sedimentation and bed formation in rivers and cooling in nuclear reactors, etc [9]. Another aspect is that inducing this coupled flow phenomena helps to achieve conditions and flow behaviour favourable for heat transfer. Researchers are continuously analyzing the behaviour experimentally and numerically.

In recognition of its numerous commercial and technological uses, the study of conducting micropolar liquids has grown in importance in recent years. Colloidal suspensions, liquid crystals, unusual lubricants, and several other industrial liquids are examples of liquids used in the design of biomedical applications. François and Eugène Cosserat, two French brothers, are credited with developing the theory of micropolar liquids in their monograph [17]. Since then, the theory has been widely accepted and has drawn attention because of its rich structure, particularly in light of [18] work. Numerous further research demonstrates its use in the rheological description of liquids having interior structure.

The reader is directed to a recent study by [19] and the references therein for a thorough analysis of the uses of micropolar liquids. The subclass of liquids known as micropolar liquids is made up of microelements that have internal structures. Numerous intriguing uses for the notion of micropolar fluids have been discovered. Sharma et al. [20] have utilized them to lubricate bearings in order to reduce skin friction and improve performance.

In comparison to the conventional fluid theories, these theories have demonstrated a better load bearing capacity [21]. According to Karvelas et al. [22] and their sources, micropolar theories offer a more comprehensive explanation for complicated fluids such as blood in human carotid arteries. It is possible to model the flow of biofluids in human ureters, intestines, and arterioles using micropolar theory and conducting liquids. Magnetization utilizing micropolar fluids has been the subject of numerous investigations. A nonlinear model of PDEs with boundary conditions for momentum, microrotation, temperature, and concentration that is subsequently numerically resolved using the spectral local linearization technique.

Khan et al. [23] looked at how magnetohydrodynamic heat transfer affected upper-convected Maxwell's flow within micropolar approach with thermal radiation and joule heating.

They calculated the angular-momentum balance equation while accounting for the microrotation of fluid particles and investigated the impact of microstructural factors on macroscopic velocity profiles and micro-rotations.

In a rotating reference frame, the study [24] examined the effects of radiation and hall current on micropolar dynamic flow. The Runge–Kutta (RK) technique of order four and the shooting approach are used to compute the solution of the resulting nonlinear ODEs. Khan et al. [25] used a finite element to study the magnetohydrodynamic micropolar flow over a rectangular channel using an iterative and numerical approach.

They found that both magnetic induction and the micro-rotational velocity of particles decrease when the micropolar coupling value increases. The impact of MMR, a naturally occurring phenomena, in promoting micropolar liquids has not been taken into account in any of these earlier investigations.

This thesis investigates the influence of micromagnetorotation on flow dynamics, focusing on the effects of various parameters such as magnetic field strength and orientation, fluid viscosity, and flow geometry.

The governing equations, which describe fluid-magnetic field interactions, are modeled in detail, accounting for magnetization, rotation, and shear forces. To solve these equations, FreeFem++ is used to implement a variational framework based on the Galerkin method.

Numerical simulations explore the impact of micromagnetorotation on velocity profiles, pressure distributions, and vorticity, revealing how different parameters affect flow stability and pattern formation.

The study provides insights into the interplay between fluid motion and magnetic effects, with potential applications in microfluidics, materials processing, and biomedical engineering. The findings lay the groundwork for further research in micromagnetorotational systems.

1.1 Thesis Contribution

This thesis revisits the classic backward-facing step problem in fluid mechanics, focusing on the application of the Navier-Stokes equations (NSE) in 2D, with a particular emphasis on micropolar flow and the inclusion of magnetohydrodynamic (MMR) effects.

The proposed extended mathematical model is formulated as a coupled system of partial differential equations (PDEs), incorporating both the micropolar and MMR effects, alongside the corresponding boundary conditions. To solve the model, a finite element numerical method is employed. The first step in solving the governing equations is to non-dimensionalize the flow dynamics equations. Following this, a weak formulation of the system is derived to enable numerical computation. This weak formulation is then implemented using the open-source finite element software FreeFEM++.

The results obtained from the numerical simulations are thoroughly analyzed and discussed, providing insights into the effects of the MMR and micropolar terms on the flow characteristics. The computational outcomes are presented in various visualizations, such as velocity and pressure profiles, as well as temperature distributions, which highlight the significant influence of the coupled effects on the overall flow behavior in the BFS configuration.

1.2 Thesis Attributes

Present thesis is structured into the following six chapters:

Chapter 2 lays the groundwork by presenting fundamental laws, key definitions, and important non-dimensional parameters for simplifying the system's analysis. It also outlines the solution methodology, providing a clear roadmap for deriving results.

Chapter 3 focuses on the analysis of laminar flow over a backward-facing step (BFS). It clearly defines boundary conditions and presents the physical model in

both dimensional and non-dimensional forms to better understand the interplay between the flow and the step's geometry.

Chapter 4 explores 2D micropolar fluid flow influenced by micromagnetorotation using the Galerkin finite element method in FreeFEM++. It focuses on how Reynolds number, micropolar parameters, and boundary conditions affect velocity and flow dynamics, emphasizing the interaction between fluid rotation and micromagnetorotation. Through non-dimensionalization, weak formulation, and visual analysis via stream functions, the study deepens understanding of micropolar fluid behavior under magnetic effects.

Chapter 5 contains the conclusion of this work.

The references for this work are listed in the Bibliography.

Chapter 2

Basic Terminologies and Finite Element Procedure

2.1 Introduction

This chapter introduces fundamental concepts in fluid mechanics, focusing on the three primary flow regimes: laminar, transitional, and turbulent. Understanding these regimes is crucial for accurately predicting and modeling fluid behavior in various engineering applications.

2.2 Backward Facing Step Flow BFSF Problem

The BFSF is a canonical fluid mechanics problem that serves as a benchmark for computational fluid dynamics (CFD) and provides valuable insights into complex flow phenomena like separation, recirculation, and reattachment.

It entails a channel's abrupt growth, leading to a complex flow field with significant pressure gradients and the formation of a recirculation zone downstream the step. This problem is extensively studied due to its relevance in various engineering applications.

2.2.1 Geometrical Representation and Key Parameters

A typical backward-facing step geometry is illustrated in Figure 2.1 [26].

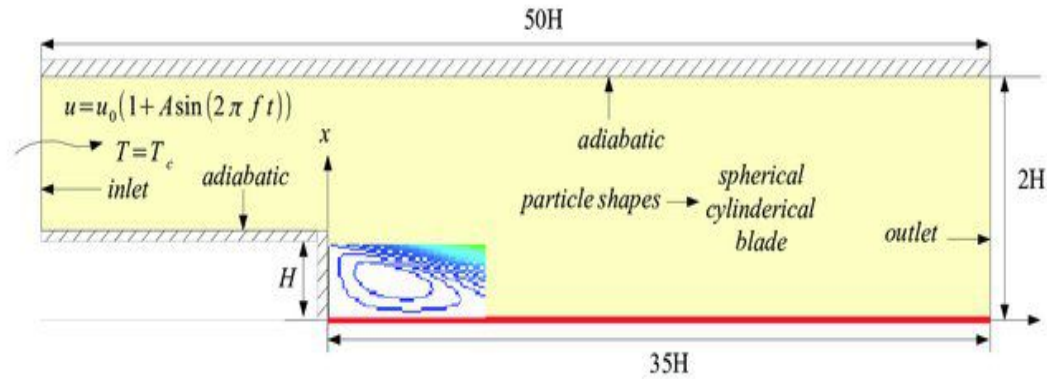


FIGURE 2.1: Backward facing step geometry

The geometrical parameters that define the backward-facing step are:

- **Step Height (H):** The vertical distance between the upstream and downstream channel walls. This is the primary geometric feature that induces flow separation.
- **Inlet Height (h):** The height of the upstream channel.
- **Expansion Ratio (ER):** The ratio of the downstream channel height to the upstream channel height ($ER = \frac{H+h}{h} = 1 + \frac{H}{h}$). This ratio significantly influences the size and characteristics of the recirculation zone.
- **Step Length (L):** The length of the step (often considered the length of the upstream section).
- **Reattachment Length (Lr):** The separation between the step edge and the lower wall where the separated flow rejoins. This metric, which depends on the Reynolds number and expansion ratio, is essential for describing the recirculation zone.

2.3 Types of Fluid Flow

The fluids may be classified as follows:

2.3.1 Uniform Flow

“The type of flow, in which the velocity at any given time does not change with respect to space is called uniform flow. Mathematically, we have:

$$\left(\frac{\partial V}{\partial s}\right)_{t=\text{constant}} = 0$$

where ∂V = Change in velocity, and ∂s = Displacement in any direction.” [27]

Example:Flow through a straight prismatic conduit (i.e. flow through a straight pipe of constant diameter).

2.3.2 Non-uniform Flow

“It is that type of flow in which the velocity at any given time changes with respect to space. Mathematically,

$$\left(\frac{\partial V}{\partial s}\right)_{t=\text{constant}} \neq 0.” [27]$$

Example:(i) Flow through a non-prismatic conduit.

(ii) Flow around a uniform diameter pipe-bend or a canal bend.

2.3.3 Steady Flow

“The type of flow in which the fluid characteristics like velocity, pressure, density, etc. at a point do not change with time is called steady flow” [27].

Example:Flow through a prismatic or non-prismatic conduit at a constant flow rate $Q\text{m}^3/\text{s}$ is steady. (A prismatic conduit has a constant size shape and has a velocity equation of the form $u = ax^2 + bx + c$, which is independent of time t).

2.3.4 Unsteady Flow

“It is that type of flow in which the velocity, pressure or density at a point change w.r.t. time”. [27]

Example:The flow in a pipe whose valve is being opened or closed gradually.

(velocity equation is in the form $u = ax^2 + bx(t)$).

2.3.5 Rotational Flow

“A flow is said to be rotational if the fluid particles while moving in the direction of flow rotate about their mass centres. Flow near the solid boundaries is rotational.” [27]

Example:Motion of liquid in a rotating tank.

2.3.6 Irrotational Flow

“A flow is said to be irrotational if the fluid particles while moving in the direction of flow do not rotate about their mass centres. Flow outside the boundary layer is generally considered irrotational.” [27]

Example: Flow above a drain hole of a stationary tank or a wash basin.

2.3.7 Laminar Flow

“A laminar flow is one in which paths taken by the individual particles do not cross one another and move along well defined paths.” [27]

Example:

- (i) Flow through a capillary tube.
- (ii) Flow of blood in veins and arteries.

2.3.8 Turbulent Flow

“A turbulent flow is that flow in which fluid particles move in a zig zag way in nature.” [27].

Example: High velocity flow in a conduit of large size. The majority of fluid flow issues that arise in engineering practice are turbulent in nature.

2.3.9 Compressible Flow

“It is that type of flow in which the density ρ of the fluid changes from point to point (or in other words density is not constant for this flow). Mathematically:

$$\rho \neq \text{constant.}” [27]$$

Example:Flow of gases through orifices, nozzles, gas turbines, etc.

2.3.10 Incompressible Flow

“It is that type of flow in which density is constant for the fluid flow. Liquids are generally considered flowing incompressibly. Mathematically:

$$\rho = \text{constant.}” [27]$$

Example: Subsonic aerodynamics.

2.4 Fundamental Laws

”The general conservation laws will be stated and specialized to the primary case of interest, nonisothermal, incompressible flows.” [28]

These laws are represented as follows.

2.4.1 The Continuity Equation

“The principle of conservation of mass can be stated as the time rate of change of mass in a fixed volume is equal to the net rate of flow of mass across the surface.

The mathematical statement of the principle results in the following equation, known as the continuity (of mass) equation

$$\frac{\partial \rho}{\partial t} + \nabla \cdot (\rho \mathbf{v}) = 0 \quad (2.1)$$

where ρ is the density of the medium, \mathbf{v} the velocity vector, and ∇ is the nabla or del operator.

The continuity equation in (2.1) is in conservation (or divergence) form since it can be derived directly from an integral statement of mass conservation.

By introducing the material derivative or Eulerian derivative operator $\frac{D}{Dt}$

$$\frac{D}{Dt} = \frac{\partial}{\partial t} + \mathbf{v} \cdot \nabla, \quad (2.2)$$

the continuity equation (2.1) can be expressed in the alternate, non-conservation (or advective) form

$$\frac{\partial \rho}{\partial t} + \mathbf{v} \cdot \nabla \rho + \rho \nabla \cdot \mathbf{v} = \frac{D\rho}{Dt} + \rho \nabla \cdot \mathbf{v} = 0 \quad (2.3)$$

For steady-state conditions, the continuity equation becomes

$$\nabla \cdot (\rho \mathbf{v}) = 0 \quad (2.4)$$

When the density changes following a fluid particle are negligible, the continuum is termed incompressible and we have $\frac{D\rho}{Dt} = 0$. The continuity equation (2.3) then becomes

$$\nabla \cdot \mathbf{v} = 0 \quad (2.5)$$

which is often referred to as the incompressibility condition or incompressibility constraint.” [28]

2.4.2 Conservation of Momentum

“The principle of conservation of linear momentum (or Newton’s Second Law of motion) states that the time rate of change of linear momentum of a given set of particles is equal to the vector sum of all the external forces acting on the particles of the set, provided Newton’s Third Law of action and reaction governs the internal forces. Newton’s Second Law can be written as

$$\frac{\partial \rho \mathbf{v}}{\partial t} + \nabla \cdot (\rho \mathbf{v} \otimes \mathbf{v}) = \nabla \cdot \boldsymbol{\sigma} + \rho \mathbf{f} \quad (2.6)$$

where \otimes is the tensor (or dyadic) product of two vectors, $\boldsymbol{\sigma}$ is the Cauchy stress tensor (N/m^2) and \mathbf{f} is the body force vector, measured per unit mass and normally taken to be the gravity vector. Equation (2.6) describes the motion of a continuous medium, and in fluid mechanics they are also known as the Navier equations.

The form of the momentum equation shown in (2.6) is the conservation (divergence) form that is most often utilized for compressible flows.

This equation may be simplified to a form more commonly used with incompressible flows. Expanding the first two derivatives and collecting terms

$$\rho \left(\frac{\partial \mathbf{v}}{\partial t} + \mathbf{v} \nabla \cdot \mathbf{v} \right) + \mathbf{v} \left(\frac{\partial \rho}{\partial t} + \nabla \cdot \rho \mathbf{v} \right) = \nabla \cdot \boldsymbol{\sigma} + \rho \mathbf{f} \quad (2.7)$$

The second term in parentheses is the continuity equation (2.1) and neglecting this term allows (2.7) to reduce to the non-conservation (advective) form

$$\rho \frac{D\mathbf{v}}{Dt} = \nabla \cdot \boldsymbol{\sigma} + \rho \mathbf{f} \quad (2.8)$$

where the material derivative (2.2) has been employed.

The principle of conservation of angular momentum can be stated as the time rate of change of the total moment of momentum of a given set of particles is equal to the vector sum of the moments of the external forces acting on the system. In the absence of distributed couples, the principle leads to the symmetry of the stress tensor:

$$\boldsymbol{\sigma} = (\boldsymbol{\sigma})^T \quad (2.9)$$

where the superscript T denotes the transpose of the enclosed quantity.” [28]

2.4.3 Conservation of Energy

“The law of conservation of energy (or the First Law of Thermodynamics) states that the time rate of change of the total energy is equal to the sum of the rate of work done by applied forces and the change of heat content per unit time. In the general case, the First Law of Thermodynamics can be expressed in conservation form as

$$\frac{\partial \rho e^t}{\partial t} + \nabla \cdot \rho \mathbf{v} e^t = -\nabla \cdot \mathbf{q} + \nabla \cdot (\boldsymbol{\sigma} \cdot \mathbf{v}) + Q + \rho \mathbf{f} \cdot \mathbf{v} \quad (2.10)$$

where $e^t = e + 1/2 \mathbf{v} \cdot \mathbf{v}$ is the total energy (J/m^3), e is the internal energy, \mathbf{q} is the heat flux vector (W/m^2) and Q is the internal heat generation (W/m^3). The total energy equation (2.10) is useful for high speed compressible flows where the kinetic energy is significant. For incompressible flows, an internal energy equation is more appropriate and can be derived from (2.10) with use of the momentum equation (2.6). Taking the dot product of the velocity vector with the momentum equation produces an equation for the kinetic energy; this equation is subtracted from the total energy equation (2.10) to produce the conservation (divergence) form of the internal energy equation

$$\frac{\partial \rho e}{\partial t} + \nabla \cdot \rho \mathbf{v} e = -\nabla \cdot \mathbf{q} + Q + \Phi \quad (2.11)$$

where Φ is a dissipation function that is defined by

$$\Phi = \boldsymbol{\sigma} : \nabla \mathbf{v} \quad (2.12)$$

In Eq. (2.12) $\nabla \mathbf{v}$ is the velocity gradient tensor which will be defined more completely in the following sections. The thermal energy equation in (2.11) can be simplified further by expanding the derivatives on the left-hand side of the equation and using the continuity equation. The resulting equation is the non-conservative (advective) form of the energy equation

$$\rho \frac{De}{Dt} = -\nabla \cdot \mathbf{q} + Q + \Phi \quad (2.13)$$

which is the standard form used for incompressible flows. Constitutive relations for e and \mathbf{q} will be defined in the next sections and allow (2.13) to be expressed in terms of the temperature T .” [28]

2.5 Heat and Mass Transfer Phenomenon and Related Properties

Heat transfer is the phenomenon of transferring energy and entropy from one place to another. The formal definition of heat transfer and its different types are given below.

2.5.1 Heat Transfer

“Heat transfer is a branch of engineering that deals with the transfer of thermal energy from one point to another within a medium or from one medium to another due to the occurrence of a temperature difference. Heat transfer may take place in one or more of its three basic forms: conduction, convection, and radiation.” [28]

2.5.2 Mass Transfer

“Mass transfer is the flow of molecules from one body to another when these bodies are in contact or within a system consisting of two components when the distribution of materials is not uniform. When a copper plate is placed on a steel plate, some molecules from either side will diffuse into the otherside. When salt is placed in a glass and water poured over it, after sufficient time the salt molecules will diffuse into the water body. ” [29]

2.5.3 Conduction

“Conduction is the transfer of heat from one part of a body at a higher temperature to another part of the same body at a lower temperature, or from one

body at a higher temperature to another body in physical contact with it at a lower temperature. The conduction process takes place at the molecular level and involves the transfer of energy from the more energetic molecules to those with a lower energy level. This can be easily visualized within gases, where we note that the average kinetic energy of molecules in the higher-temperature regions is greater than that of those in the lower-temperature regions.” [30]

2.5.4 Convection

“The process of heat transfer between a surface and a fluid flowing in contact with it is called convection.” [29]

2.5.5 Natural Convection or Free Convections

“If the flow is caused by the buoyant forces generated by heating or cooling of the fluid the process is called as natural or freeconvection.” [29]

2.5.6 Forced Convection

“If the flow is caused by an external device like a pump or blower, it is termed as forced convection.” [29]

2.5.7 Radiation

“Radiation, or more correctly thermal radiation, is electromagnetic radiation emitted by a body by virtue of its temperature and at the expense of its internal energy.

Thus thermal radiation is of the same nature as visible light, x -rays, and radio waves, the difference between them being in their wavelengths and the source of generation. The eye is sensitive to electromagnetic radiation in the region from 0.39 to $0.78\mu m$; this is identified as the visible region of the spectrum. Radio waves have a wavelength of 1×10^3 to $2 \times 10^{10}\mu m$, and x -rays have wavelengths of

1×10^{-5} to $2 \times 10^{-2} \mu m$, while the bulk of thermal radiation occurs in rays from approximately 0.1 to $100 \mu m$.” [30]

2.6 Dimensionless Parametres

The dimensionless parameter explained in the following:

2.6.1 Reynolds Number

“It is the most significant dimensionless number which is used to identify the different flow behaviors like laminar or turbulent flow. Mathematically, it is expressed as

$$Re = \frac{LU}{\nu}$$

where U denotes the free stream velocity, L is the characteristic length and ν stands for kinematic viscosity.” [31]

2.7 Finite Element Method

FEM has become a crucial technique for addressing intricate physical problems governed by partial differential equations (PDEs) and integro-differential equations, especially within the domains of science and engineering. With its development during the 1950s, FEM revolutionized the way engineers and scientists approached the analysis and simulation of physical systems.

The method’s breakthrough came with the availability of powerful computers, enabling the numerical solution of otherwise intractable problems. FEM discretizes a large problem into smaller, manageable parts, or elements, and uses variational principles and numerical techniques to obtain approximate solutions. This flexibility has made it a versatile method, applicable to a wide range of fields such

as solid mechanics, fluid dynamics, structural analysis, heat transfer, electromagnetism, and more.

Furthermore, FEM is essential in modern design processes, where it is used to predict the behavior of structures, optimize designs, and conduct simulations that are otherwise difficult or impossible to perform in real life.

As the complexity of systems and models continues to increase, FEM remains a powerful and reliable tool, driving advancements in engineering analysis, material science, and other related domains.

2.8 Galerkin Finite Element Method for Nonlinear PDEs

The Galerkin based FEM is a powerful numerical technique for solving Nonlinear PDEs with associated boundary conditions. The method proceeds in several key steps:

2.8.1 Weak Formulation

The first step involves deriving the weak formulation of the governing equations. This is achieved by multiplying the PDE with test functions (also known as weight functions), denoted by v , and integrating over the problem domain, Ω .

This process can be represented generically as:

$$\int_{\Omega} \mathcal{L}(u)v \, d\Omega = \int_{\Omega} f v \, d\Omega,$$

where $\mathcal{L}(u)$ represents the differential operator, u is the unknown solution, and f is the source term. The weak formulation reduces the order of differentiation required, making it easier to find approximate solutions.

2.8.2 Galerkin Approximation

The solution u , is approximated as:

$$u \approx u^h = \sum_{i=1}^n N_i \phi_i(x),$$

where N_i are the unknown coefficients and the symbol n represents the number of test functions. These basis functions are typically polynomials chosen to satisfy the essential boundary conditions of the problem.

Crucially, in the Galerkin method, the basis v are chosen to be the same as the basis functions, i.e., $v = \phi_j$.

2.8.3 Discretization

Substituting the Galerkin approximation into the weak formulation guide to a discretized system of equations. This involves integrating terms like:

$$\int_{\Omega} \mathcal{L} \left(\sum_{i=1}^n N_i \phi_i \right) \phi_j d\Omega = \int_{\Omega} f \phi_j d\Omega, \quad j = 1, 2, \dots, n.$$

Due to the nonlinearity of \mathcal{L} , this often results in a nonlinear system of algebraic equations for the coefficients N_i .

2.8.4 Element Formulation and Assembly

The problem geometry is divided into broken down to smaller elements, and the weak formulation is applied to each element. This results in element-level equations.

These element equations are then assembled together to form a global system of equations that represents the entire problem. The assembly process incorporates the connectivity between elements and the boundary conditions.

2.9 Variational Formulation

The core idea behind the variational formulation is to shift the focus from finding a solution that satisfies the governing differential equation *pointwise* (the strong form) to finding a numerical solution which satisfy the equation *in a weighted average sense* over the entire problem geometry (the weak form).

This “weighted average” is achieved through integration and the use of test functions.

The breakdown of the process is given below:

1. **Test Functions:** These functions, often denoted by v or w , belong to a carefully chosen function space (e.g., Sobolev space). They are crucial in “testing” the equation and extracting information about the solution. They often have specific properties, like being zero on the domain’s boundary.
2. **Weak Formulation:** The original differential equation (the strong form) is multiplied by a test function and integrated over the entire domain. Integration by parts is often employed to reduce the order of differentiation required on the solution (transferring it to the test function).

This results in the weak form, which is an integral equation. The weak form relaxes the differentiability requirements of the numerical solution compared to the strong form of the problem. This is a key advantage, as it allows us to consider a broader class of functions as potential solutions.

3. **Trial Functions:** To find an approximate solution, we introduce trial functions (often denoted by u or ϕ). These functions are also chosen from a suitable function space and are used to represent the approximate solution. They are often stated as linear combination of test functions, each with an unknown coefficient. These basis functions can be globally defined (e.g., polynomials) or locally defined (e.g., piecewise polynomials used in finite element methods).
4. **Galerkin Method:** A very common approach is the Galerkin method, where the trial functions and basis functions are selected from the *same*

function space. This simplifies the problem and often leads to good approximations.

5. **Discretization:** Substituting the trial functions into the weak form results in a system of equations for the unknown coefficients of the test functions. The size of this system depends on the number of test functions used. Solving this system yields the approximate solution.
6. **Approximation:** The accuracy of the approximate solution depends on the choice of test and trial functions, the number of test functions used, and the properties of the function space. By increasing the number of test functions (and thus the size of the algebraic system), we can often improve the accuracy of the approximation.

Finite Element Method (FEM) is a powerful technique that utilizes the variational formulation is the FEM. In FEM, the domain is divided into smaller elements, and piecewise polynomial basis functions are used within each element. This allows for greater flexibility in handling complex geometries and material properties.

2.10 2D Example: Heat Equation

Consider the heat equation in 2D as below

$$\frac{\partial^2 u}{\partial x^2} + \frac{\partial^2 u}{\partial y^2} = f(x, y) \quad \text{in } \Omega \quad u = 0 \quad \text{on } \partial\Omega, \quad (2.14)$$

where u is the temperature, f is the heat source, Ω is the domain, and $\partial\Omega$ is the boundary. The steps in solving Eq.(2.22) are as follows:

1. Choose a test function and multiply the model equation and integrate by parts:

$$\int_{\Omega} \left(\frac{\partial u}{\partial x} \frac{\partial v}{\partial x} + \frac{\partial u}{\partial y} \frac{\partial v}{\partial y} \right) dx dy = \int_{\Omega} f v dx dy. \quad (2.15)$$

2. Divide the domain Ω into triangular elements.

3. Choose linear basis functions φ_i such that $\varphi_i(x_i, y_i) = 1$ and $\varphi_i(x_j, y_j) = 0$ for $i \neq j$, where (x_i, y_i) are the nodes of the elements.
4. Approximate solution as $u \approx \sum_i u_i \varphi_i$ is used to substitute into the weak form to get:

$$\int_{\Omega} \left(\sum_i u_i \frac{\partial \varphi_i}{\partial x} \frac{\partial \varphi_j}{\partial x} + \sum_i u_i \frac{\partial \varphi_i}{\partial y} \frac{\partial \varphi_j}{\partial y} \right) dx dy = \int_{\Omega} f \varphi_j dx dy, \quad (2.16)$$

for all basis functions φ_j .

5. Assemble the element-level equations into a system of global equations:

$$[K]\{u\} = \{F\}, \quad (2.17)$$

where the system stiffness matrix is represented by $[K]$, $\{u\}$ is the vector of unknown coefficients, and $\{F\}$ is load vector.

6. Solve the obtained system of algebraic equations for the unknown $\{u\}$.
7. The approximate solution is given by $u \approx \sum_i u_i \varphi_i$.

2.11 Advantages of Galerkin FEM

The advantages of Galerkin FEM are as follows:

1. **Accuracy:** Can achieve high accuracy with relatively few elements.
2. **Flexibility:** Can handle complex geometries and boundary conditions.
3. **Versatility:** Applicable to a wide range of problems in engineering and physics.

2.12 Limitations of Galerkin FEM

The limitations of Galerkin FEM are as follows:

1. **Computational Cost:** Can be computationally expensive for large problems.
2. **Mesh Dependence:** Accuracy depends on the quality of the mesh.
3. **Complexity:** Implementation can be complex, especially for higher-order elements and complex geometries.

Chapter 3

Laminar Flow Over a Backward Facing Step

3.1 Introduction

In this chapter, we present a detailed analysis of laminar flow over a Backward Facing Step geometry. To begin with, the governing partial differential equations (PDEs) were transformed from their dimensional form into a dimensionless form to simplify the mathematical model for numerical computation.

Following this, the equations were converted into their weak form, which is essential for implementing the Galerkin Finite Element Method. As part of the overall analysis of the flow behavior within this geometry under laminar conditions, numerical results were obtained and further visualized through graphical representations.

Streamlines were plotted to illustrate the flow patterns and velocity distributions, providing valuable insights into the hydrodynamic characteristics of the Backward Facing Step geometry.

3.2 Geometry of the Problem

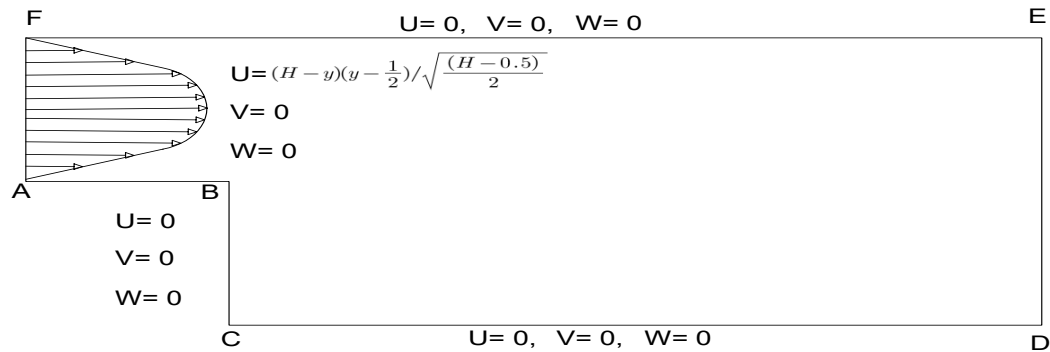


FIGURE 3.1: Backward facing step flow Configuration.

3.3 Dimensional Form of the Governing Equations

This section outlines the governing equations for the fluid flow problem in their dimensional form. The velocity vector $\mathbf{u} = (u, v)$, where u represents component of velocity in x -direction and v represents component of velocity in y -direction. The pressure is denoted by p .

- **Continuity Equation (Conservation of Mass):**

$$\frac{\partial u}{\partial x} + \frac{\partial v}{\partial y} = 0 \quad (3.1)$$

This equation states that the rate of change of fluid volume within a control volume must be zero for an incompressible fluid. In other words, the amount of fluid entering the control volume must equal the amount of fluid leaving.

- **Momentum Equation for u -velocity (Conservation of x -momentum):**

$$\rho \left(u \frac{\partial u}{\partial x} + v \frac{\partial u}{\partial y} \right) = -\frac{\partial p}{\partial x} + \mu \left(\frac{\partial^2 u}{\partial x^2} + \frac{\partial^2 u}{\partial y^2} \right) \quad (3.2)$$

The L.H.S of the equation represents the inertial effects (convective terms), whereas the R.H.S accounts for the contributions from pressure and viscous forces.

ρ is the density and μ is the dynamic viscosity of the fluid.

- **Momentum Equation for v -velocity (Conservation of y -momentum):**

$$\rho \left(u \frac{\partial v}{\partial x} + v \frac{\partial v}{\partial y} \right) = - \frac{\partial p}{\partial y} + \mu \left(\frac{\partial^2 v}{\partial x^2} + \frac{\partial^2 v}{\partial y^2} \right) \quad (3.3)$$

This equation is analogous to the u -momentum equation, but it describes the conservation of momentum in the y -direction.

The terms have the same physical interpretations as in the u -momentum equation.

3.4 Dimensional Boundary Conditions

Dimensional boundary conditions of the problem are:

- At inlet (A-K):

$$u = (H - y)(y - \frac{1}{2}) / \sqrt{(H - 0.5)/2}, \quad v = 0.$$

- At the walls (A-B, B-C, C-D and K-F):

$$u = 0, \quad v = 0.$$

- At outlet (D-F):

$$\frac{\partial u}{\partial x} = 0, \quad \frac{\partial v}{\partial x} = 0.$$

3.4.1 Dimensionless Governing Equations with Boundary Conditions

Following are the transformation parameters for the physical laws to convert them into the dimensionless form:

$$u = \frac{U}{U_{max}}, \quad v = \frac{V}{U_{max}}, \quad x = \frac{X}{H-h}, \quad y = \frac{Y}{H-h},$$

$$p = \frac{p}{\rho U_{max}^2} \quad \text{and} \quad Re = \frac{(H-h)U_{max}}{\nu}.$$

The Eq. (3.1)-(3.3) are converted into non-dimensional form as follows: Let us denote $H-h=L$. then

- $X = \frac{x}{L} \Rightarrow \frac{\partial X}{\partial x} = \frac{1}{L}$
- $Y = \frac{y}{L} \Rightarrow \frac{\partial Y}{\partial y} = \frac{1}{L}$
- $U = \frac{u}{u_o} \Rightarrow u = u_o U$
- $V = \frac{v}{u_o} \Rightarrow v = u_o V$
- $\frac{\partial u}{\partial x} = \frac{\partial u}{\partial X} \frac{\partial X}{\partial x} = \frac{\partial}{\partial X} (u) \frac{1}{L} = \frac{\partial}{\partial X} (u_o U) \frac{1}{L} = \frac{u_o}{L} \frac{\partial U}{\partial X}$
- $\frac{\partial u}{\partial y} = \frac{\partial u}{\partial Y} \frac{\partial Y}{\partial y} = \frac{\partial}{\partial Y} (u) \frac{1}{L} = \frac{\partial}{\partial Y} (u_o U) \frac{1}{L} = \frac{u_o}{L} \frac{\partial U}{\partial Y}$
- $\frac{\partial v}{\partial y} = \frac{\partial v}{\partial Y} \frac{\partial Y}{\partial y} = \frac{\partial}{\partial Y} (v) \frac{1}{L} = \frac{\partial}{\partial Y} (u_o V) \frac{1}{L} = \frac{u_o}{L} \frac{\partial V}{\partial Y}$
- $u \frac{\partial u}{\partial x} = u_o U \frac{u_o}{L} \frac{\partial U}{\partial X} = \frac{u_o^2}{L} U \frac{\partial U}{\partial X}$
- $v \frac{\partial u}{\partial y} = u_o V \frac{u_o}{L} \frac{\partial U}{\partial Y} = \frac{u_o^2}{L} V \frac{\partial U}{\partial Y}$
- $\frac{\partial v}{\partial x} = \frac{\partial v}{\partial X} \frac{\partial X}{\partial x} = \frac{\partial}{\partial X} (v) \frac{1}{L} = \frac{\partial}{\partial X} (u_o V) \frac{1}{L} = \frac{u_o}{L} \frac{\partial V}{\partial X} = u_o U \frac{u_o}{L} \frac{\partial V}{\partial X} = \frac{u_o^2}{L} U \frac{\partial V}{\partial X}$
- $v \frac{\partial v}{\partial y} = u_o V \frac{u_o}{L} \frac{\partial V}{\partial Y} = \frac{u_o^2}{L} V \frac{\partial V}{\partial Y}$

Now, the dimensionless form of the continuity equation (3.1) can be obtained as follows,

$$\begin{aligned}\frac{\partial u}{\partial x} + \frac{\partial v}{\partial y} &= 0, \\ \frac{u_o}{L} \frac{\partial U}{\partial X} + \frac{u_o}{L} \frac{\partial V}{\partial Y} &= 0, \\ \frac{u_o}{L} \left(\frac{\partial U}{\partial X} + \frac{\partial V}{\partial Y} \right) &= 0,\end{aligned}$$

As $\frac{u_o}{L} \neq 0$ but,

$$\frac{\partial U}{\partial X} + \frac{\partial V}{\partial Y} = 0. \quad (3.4)$$

The dimensionless form of the u -momentum equation (3.2) can be obtained as follows,

$$\begin{aligned}u \frac{\partial u}{\partial x} + v \frac{\partial u}{\partial y} &= -\frac{1}{\rho} \frac{\partial p}{\partial x} + \frac{1}{\rho} \mu \left(\frac{\partial^2 u}{\partial x^2} + \frac{\partial^2 u}{\partial y^2} \right), \\ \frac{u_o^2}{L} U \frac{\partial U}{\partial X} + \frac{u_o^2}{L} V \frac{\partial U}{\partial Y} &= -\frac{1}{\rho} \frac{\partial p}{\partial x} + \frac{1}{\rho} \mu \left(\frac{u_o}{L^2} \frac{\partial^2 U}{\partial X^2} + \frac{u_o}{L^2} \frac{\partial^2 U}{\partial Y^2} \right), \\ \frac{u_o^2}{L} \left[U \frac{\partial U}{\partial X} + V \frac{\partial U}{\partial Y} \right] &= -\frac{1}{\rho} \frac{\partial p}{\partial x} + \frac{\mu}{\rho} \frac{u_o}{L^2} \left(\frac{\partial^2 U}{\partial X^2} + \frac{\partial^2 U}{\partial Y^2} \right), \\ U \frac{\partial U}{\partial X} + V \frac{\partial U}{\partial Y} &= -\frac{L}{u_o^2} \frac{1}{\rho} \frac{\partial p}{\partial x} + \frac{L\mu}{\rho u_o^2} \frac{u_o}{L^2} \left(\frac{\partial^2 U}{\partial X^2} + \frac{\partial^2 U}{\partial Y^2} \right), \\ U \frac{\partial U}{\partial X} + V \frac{\partial U}{\partial Y} &= -\frac{L}{u_o^2} \frac{1}{\rho} \frac{\partial}{\partial X} \frac{\partial X}{\partial x} (p) + \frac{\mu}{L\rho u_o} \left(\frac{\partial^2 U}{\partial X^2} + \frac{\partial^2 U}{\partial Y^2} \right) \\ U \frac{\partial U}{\partial X} + V \frac{\partial U}{\partial Y} &= \frac{1}{\frac{\rho L u_o}{\mu}} \left(\frac{\partial^2 U}{\partial X^2} + \frac{\partial^2 U}{\partial Y^2} \right) - L \frac{\partial}{\partial X} \frac{1}{L} \left(\frac{p}{\rho u_o^2} \right), \\ U \frac{\partial U}{\partial X} + V \frac{\partial U}{\partial Y} &= \frac{1}{Re} \left(\frac{\partial^2 U}{\partial X^2} + \frac{\partial^2 U}{\partial Y^2} \right) - \frac{\partial P}{\partial X},\end{aligned} \quad (3.5)$$

Similarly, the dimensionless form of the v -momentum equation (3.3) can be obtained as follows,

$$u \frac{\partial v}{\partial x} + v \frac{\partial v}{\partial y} = -\frac{1}{\rho} \frac{\partial p}{\partial y} + \frac{1}{\rho} \mu \left(\frac{\partial^2 v}{\partial x^2} + \frac{\partial^2 v}{\partial y^2} \right),$$

$$\begin{aligned}
\frac{u_o^2}{L}U \frac{\partial V}{\partial X} + \frac{u_o^2}{L}V \frac{\partial V}{\partial Y} &= -\frac{1}{\rho} \frac{\partial p}{\partial y} + \frac{1}{\rho} \mu \left(\frac{u_o}{L^2} \frac{\partial^2 V}{\partial X^2} + \frac{u_o}{L^2} \frac{\partial^2 V}{\partial Y^2} \right) \\
\frac{u_o^2}{L} \left[U \frac{\partial V}{\partial X} + V \frac{\partial V}{\partial Y} \right] &= -\frac{1}{\rho} \frac{\partial p}{\partial y} + \frac{\mu}{\rho L^2} \left(\frac{\partial^2 V}{\partial X^2} + \frac{\partial^2 V}{\partial Y^2} \right), \\
\frac{\partial V}{\partial T} + U \frac{\partial V}{\partial X} + V \frac{\partial V}{\partial Y} &= -\frac{L}{u_o^2} \frac{1}{\rho} \frac{\partial p}{\partial y} + \frac{L}{u_o^2} \frac{\mu}{\rho L^2} \left(\frac{\partial^2 V}{\partial X^2} + \frac{\partial^2 V}{\partial Y^2} \right), \\
\frac{\partial V}{\partial T} + U \frac{\partial V}{\partial X} + V \frac{\partial V}{\partial Y} + \frac{L}{u_o^2} \frac{1}{\rho} \frac{\partial}{\partial Y} \frac{\partial}{\partial Y} (p) &= \frac{\mu}{\rho L u_o} \left(\frac{\partial^2 V}{\partial X^2} + \frac{\partial^2 V}{\partial Y^2} \right), \\
U \frac{\partial V}{\partial X} + V \frac{\partial V}{\partial Y} &= -L \frac{\partial}{\partial Y} \frac{1}{L} \left(\frac{p}{\rho u_o^2} \right) + \frac{1}{\frac{\rho L u_o}{\mu}} \left(\frac{\partial^2 V}{\partial X^2} + \frac{\partial^2 V}{\partial Y^2} \right), \\
U \frac{\partial V}{\partial X} + V \frac{\partial V}{\partial Y} + \frac{\partial P}{\partial Y} &= \frac{1}{Re} \left(\frac{\partial^2 V}{\partial X^2} + \frac{\partial^2 V}{\partial Y^2} \right),
\end{aligned}$$

After above discussion the Eq. (3.1)-(3.3) are transformed to:

$$\frac{\partial U}{\partial X} + \frac{\partial V}{\partial Y} = 0, \quad (3.6)$$

$$U \frac{\partial U}{\partial X} + V \frac{\partial U}{\partial Y} = -\frac{\partial P}{\partial X} + \frac{1}{Re} \left(\frac{\partial^2 U}{\partial X^2} + \frac{\partial^2 U}{\partial Y^2} \right), \quad (3.7)$$

and

$$U \frac{\partial V}{\partial X} + V \frac{\partial V}{\partial Y} = -\frac{\partial P}{\partial Y} + \frac{1}{Re} \left(\frac{\partial^2 V}{\partial X^2} + \frac{\partial^2 V}{\partial Y^2} \right), \quad (3.8)$$

These equations represent the dimensionless form of the NSE for an incompressible, two-dimensional fluid flow. Equation (3.7) is the Momentum Equation in X-direction which expresses the conservation of momentum in X-direction. The terms involved in Equation (3.7) are described below.

The term, $U \frac{\partial U}{\partial X} + V \frac{\partial U}{\partial Y}$, is the convective (or advective) term. The term $-\frac{\partial P}{\partial X}$, is the gradient of pressure field. A pressure gradient drives the flow.

The term $\frac{1}{Re} \left(\frac{\partial^2 U}{\partial X^2} + \frac{\partial^2 U}{\partial Y^2} \right)$, is the viscous term.

Equation (3.8) is the momentum equation in the Y-direction is analogous to Equation (3.7), but it expresses the conservation of momentum in the Y-direction.

The Reynolds number (Re) naturally appears in this dimensionless form and plays a crucial role in determining the flow regime (laminar or turbulent). Equations (3.6), (3.7), and (3.8) together form the core of fluid dynamics.

Non-Dimensional Boundary Conditions

The associated dimensionless boundary conditions on the problem geometry are given as:

- At inlet (A-K):

$$U = (H - Y)(Y - \frac{1}{2})/\sqrt{(H - 0.5)/2}, \quad V = 0.$$

- At the walls (A-B, B-C, C-D and K-F):

$$U = 0, \quad V = 0.$$

- At outlet (D-F):

$$\frac{\partial U}{\partial X} = 0, \quad \frac{\partial V}{\partial X} = 0.$$

3.5 Weak formulation of the Problem

The weak formulation of the partial differential equations in Eqs. (3.6) - (3.8) are calculated as follows.

$$\begin{aligned} & \left[\left(U \frac{\partial U}{\partial X} \right) + \left(V \frac{\partial U}{\partial Y} \right) \right] \tilde{U} - q \frac{\partial}{\partial X} (U \tilde{U}) + q U \frac{\partial \tilde{U}}{\partial X} = - \frac{\partial}{\partial X} (P \tilde{U}) + P \frac{\partial \tilde{U}}{\partial X} + \frac{1}{Re} \\ & \quad \left\{ \frac{\partial^2 U}{\partial X^2} + \frac{\partial^2 U}{\partial Y^2} \right\} \tilde{U}, \\ & \int_{\Omega^n} \left[\left(U \frac{\partial U}{\partial X} \right) + \left(V \frac{\partial U}{\partial Y} \right) \right] \tilde{U} d\Omega - q \int_{\Omega^n} \frac{\partial}{\partial X} (U \tilde{U}) d\Omega + q \int_{\Omega^n} U \frac{\partial \tilde{U}}{\partial X} d\Omega = \\ & - \int_{\Omega^n} \frac{\partial}{\partial X} (P \tilde{U}) d\Omega + P \int_{\Omega^n} \frac{\partial \tilde{U}}{\partial X} d\Omega + \frac{1}{Re} \int_{\Omega^n} \left\{ \frac{\partial^2 U}{\partial X^2} + \frac{\partial^2 U}{\partial Y^2} \right\} \tilde{U} d\Omega, \end{aligned} \quad (3.9)$$

since

$$\begin{aligned} & \int_{\Omega} \psi \Delta \phi \, d\Omega = - \int_{\Omega} \nabla \phi \nabla \psi \, d\Omega + \int_{\Omega} \psi (\nabla \phi \cdot n) \, d\Gamma \\ & \psi = \tilde{U}, \quad \Delta \phi = \frac{\partial^2 U}{\partial X^2}, \quad \Delta \phi = \frac{\partial^2 U}{\partial Y^2}, \quad \nabla \phi = \frac{\partial U}{\partial X}, \quad \nabla \phi = \frac{\partial U}{\partial Y}, \quad \nabla \psi = \frac{\partial \tilde{U}}{\partial X}, \quad \nabla \psi = \frac{\partial \tilde{U}}{\partial Y} \end{aligned}$$

as

$$\nabla\phi n = \frac{\partial\phi}{\partial n} = n_x \frac{\partial\phi}{\partial X} + n_y \frac{\partial\phi}{\partial Y} \quad (\phi = U)$$

therefore

$$\begin{aligned} & \frac{1}{Re} \int_{\Omega^n} \left\{ \frac{\partial^2 U}{\partial X^2} + \frac{\partial^2 U}{\partial Y^2} \right\} \tilde{U} d\Omega = \\ & \frac{1}{Re} \left\{ - \int_{\Omega^n} \frac{\partial U}{\partial X} \frac{\partial \tilde{U}}{\partial X} d\Omega + \oint_{\Gamma} \tilde{U} \left(n_x \frac{\partial U}{\partial X} \right) d\Gamma - \int_{\Omega} \frac{\partial U}{\partial Y} \frac{\partial \tilde{U}}{\partial Y} d\Omega + \oint_{\Gamma} \tilde{U} \left(n_y \frac{\partial U}{\partial Y} \right) d\Gamma \right\} \end{aligned}$$

Now (3.7) becomes as

$$\begin{aligned} & \int_{\Omega^n} \left(U^n \circ X^n \right) \tilde{U} d\Omega + q \int_{\Omega^n} U \frac{\partial \tilde{U}}{\partial X} d\Omega = P \int_{\Omega^n} \frac{\partial \tilde{U}}{\partial X} d\Omega + \frac{1}{Re} \left\{ - \int_{\Omega^n} \right. \\ & \left. \frac{\partial U}{\partial X} \frac{\partial \tilde{U}}{\partial X} d\Omega + \oint_{\Gamma} \tilde{U} \left(n_x \frac{\partial U}{\partial X} \right) d\Gamma - \int_{\Omega} \frac{\partial U}{\partial Y} \frac{\partial \tilde{U}}{\partial Y} d\Omega + \oint_{\Gamma} \right. \\ & \left. \tilde{U} \left(n_y \frac{\partial U}{\partial Y} \right) d\Gamma \right\}, \end{aligned}$$

which is weak form of u -component of momentum equation. Similarly the weak form of the Equation (3.8) is

$$\begin{aligned} & \int_{\Omega^{n+1}} \frac{1}{\delta t} \left(V^n \circ Y^n \right) \tilde{V} d\Omega + q \int_{\Omega^{n+1}} V^{n+1} \frac{\partial \tilde{V}}{\partial Y^{n+1}} d\Omega - P^{n+1} \int_{\Omega^{n+1}} \frac{\partial \tilde{V}}{\partial Y^{n+1}} d\Omega - \\ & \frac{1}{Re} \left\{ - \int_{\Omega^{n+1}} \frac{\partial V^{n+1}}{\partial X^{n+1}} \frac{\partial \tilde{V}}{\partial X^{n+1}} d\Omega + \oint_{\Gamma} \tilde{V} \left(n_x \frac{\partial V^{n+1}}{\partial X^{n+1}} \right) d\Gamma - \int_{\Omega^{n+1}} \frac{\partial V^{n+1}}{\partial Y^{n+1}} \frac{\partial \tilde{V}}{\partial Y^{n+1}} d\Omega \right. \\ & \left. + \oint_{\Gamma} \tilde{V} \left(n_y \frac{\partial V^{n+1}}{\partial Y^{n+1}} \right) d\Gamma \right\}, \end{aligned}$$

3.6 Numerical Results and Discussion

In this section, the numerical results are presented and discussed for the model problem presented in previous sections. The weak form presented in previous section is implemented in FreeFem++ and the problem is analyzed with the geometry and boundary conditions as in Section 3.2. The results are calculated for the Reattachment lengths in the considered domain. Also, the maximum value of

the stream function is computed for varying Reynold numbers. The results are shown in the form of tables as shown below.

Re	Reattachment length
50	2.09327
150	5.07213
300	8.3155
400	9.91214
500	11.0214

TABLE 3.1: Reattachment length with varying Re.

Re	Ψ_{max}
50	0.0137976
150	0.0199193
300	0.0214554
400	0.0218086
500	0.0219075

TABLE 3.2: Maximum Stream function values with varying Re.

In Table 3.1 the Reattachment lengths are computed. In these numerical experiments the Reynold number is varied from a value $Re = 50$ to $Re = 500$. It is observed that with increasing value of the Reynolds number the Reattachment length is increasing. This is certainly because with the increasing value of the Reynold number which increase the speed of the flow. Due to increase in the speed of the flow the Reattachment point in the domain moves away form the step and therefore the Reattachment length increases.

In Table 3.2 the maximum values of the stream function are shown where the Reynold number is varied from $Re = 50$ to $Re = 500$. It is seen that with increase in the Reynold number the maximum value of the stream function also increases.

This is due to the increase velocity in the medium due to increase Reynold number and therefore the stream function values increase. In Figure 3.2, the velocity contours computed for varying values of the Reynolds number are shown. The Reynold number is varied between 50 and 500.

It is aimed at observing how increasing the flow speed affects the formation of the vortex at the backward facing step.

The flow speed within the domain increases as the Reynolds number is increased. It is seen that with increasing flow speed, the length of reattachment increases.

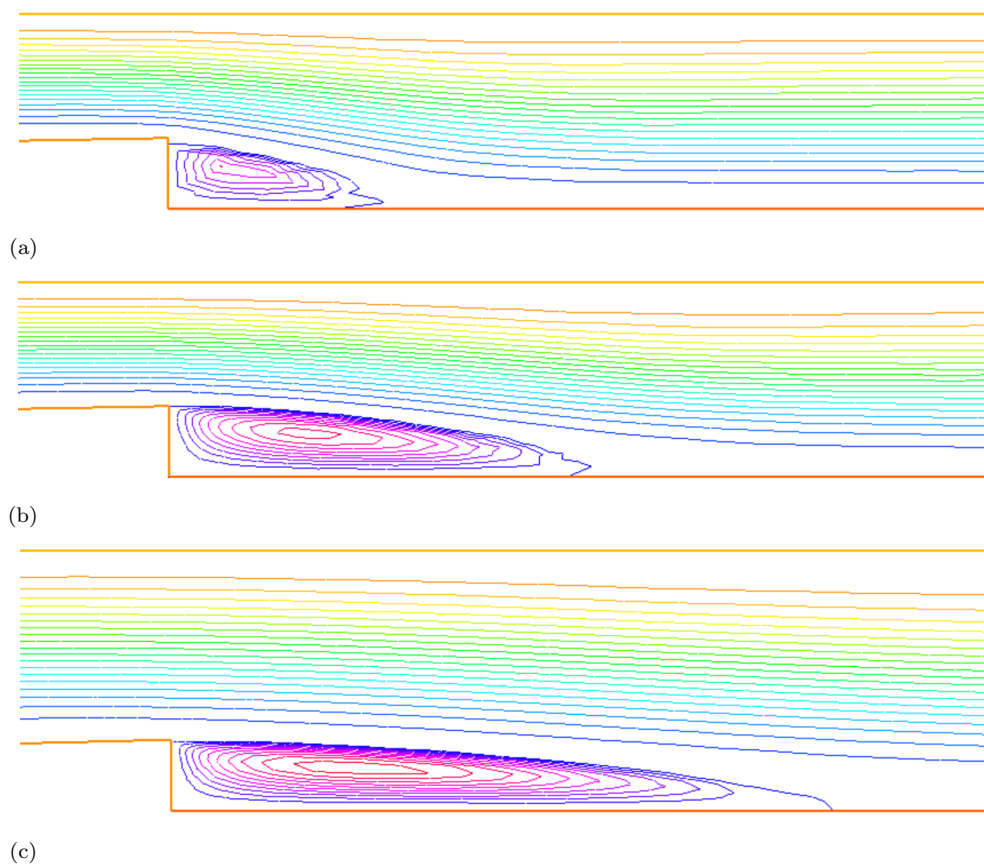


FIGURE 3.2: Velocity contours for varying Re . (a) For $Re = 50$ (b) For $Re = 150$ (c) For $Re = 500$

In Figure 3.3, the velocity contours are shown for varying values of the channel inlet height.

The Reynold number chosen for these numerical simulations is $Re = 50$. It is aimed at how the inlet height affects the formation of the velocity vortex at the step and the reattachment length.

It is seen that with increasing the channel's inlet height, the reattachment length increases.

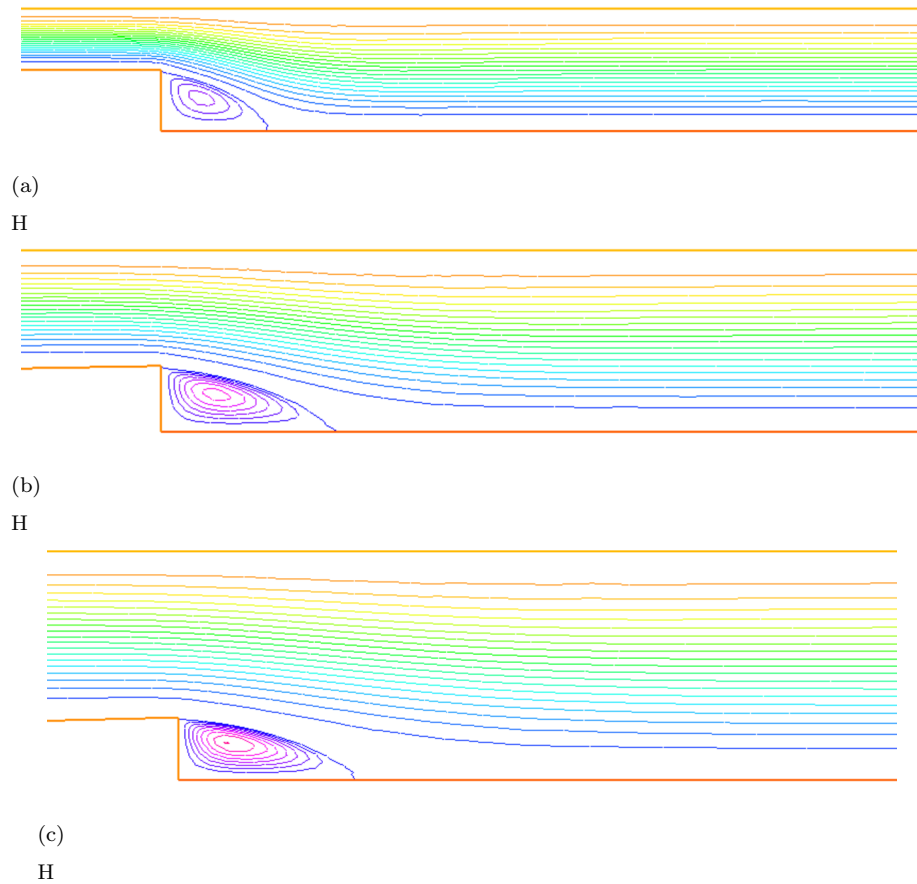


FIGURE 3.3: Velocity contours for varying channel's inlet height. (a) For $H = 1$
(b) For $H = 1.5$ (c) For $H = 2$.

Chapter 4

Backward Facing Step Micropolar Flow with Micromagnetorotation

4.1 Introduction

This chapter presents a focused study of laminar micropolar flow with micromagnetorotation effects over a Backward Facing Step geometry. The governing partial differential equations (PDEs) are nondimensionalized and reformulated into their weak form for implementation via the Galerkin Finite Element Method. Micromagnetorotation, arising from the interaction between microstructural particle spins and an external magnetic field, introduces additional body couples that modify the flow behavior. Numerical simulations reveal that micromagnetorotation enhances rotational motion, affects flow separation, and alters the reattachment length behind the step. Streamline and velocity contour plots are used to illustrate the impact of these effects on the hydrodynamics of the configuration.

4.2 Dimensional Governing Equations

In fluid mechanics, when studying flow over a BFS, key equations governing the dynamics include the continuity equation, the momentum equation, and the micromagnetorotational (MMR) equation. The continuity equation ensures mass

conservation, the momentum equation describes the fluid's motion under various forces, and the MMR equation governs the interaction between a magnetic field and a rotating fluid flow, often influenced by external magnetic fields. These equations are typically presented in their dimensional form to model the behavior of the fluid in such scenarios. Continuity Equation

$$\frac{\partial u}{\partial x} + \frac{\partial v}{\partial y} = 0, \quad (4.1)$$

Momentum equation for u -velocity

$$\frac{\partial u}{\partial t} + u \frac{\partial u}{\partial x} + v \frac{\partial u}{\partial y} = -\frac{1}{\rho} \frac{\partial p}{\partial x} + \frac{1}{\rho} (\mu + k) \left(\frac{\partial^2 u}{\partial x^2} + \frac{\partial^2 u}{\partial y^2} \right) + \frac{k}{\rho} \frac{\partial w}{\partial y} + v B_x B_y - u B_y^2, \quad (4.2)$$

Momentum equation for v -velocity

$$\frac{\partial v}{\partial t} + u \frac{\partial v}{\partial x} + v \frac{\partial v}{\partial y} = -\frac{1}{\rho} \frac{\partial p}{\partial y} + \frac{1}{\rho} (\mu + k) \left(\frac{\partial^2 v}{\partial x^2} + \frac{\partial^2 v}{\partial y^2} \right) - \frac{k}{\rho} \frac{\partial w}{\partial x} + u B_x B_y - v B_x^2, \quad (4.3)$$

Micropolar equation

$$\frac{\partial w}{\partial t} + u \frac{\partial w}{\partial x} + v \frac{\partial w}{\partial y} = \frac{1}{\rho} (\mu + k) \left(\frac{\partial^2 w}{\partial x^2} + \frac{\partial^2 w}{\partial y^2} \right) + \frac{2v_r}{\rho j} \left(\frac{\partial v}{\partial x} - \frac{\partial u}{\partial y} - 2w \right). \quad (4.4)$$

The specific boundary conditions used in this study are as follows:

- At inlet (A-F):

$$u = (H - y)(y - \frac{1}{2}) / \sqrt{(H - 0.5)/2}, \quad v = 0, \quad w = 0$$

- At the walls (A-B, B-C, C-D and E-F):

$$u = 0, \quad v = 0, \quad w = 0.$$

- At outlet (E-D):

$$\frac{\partial u}{\partial x} = \frac{\partial v}{\partial x} = 0, \quad \text{and} \quad \frac{\partial w}{\partial x} = 0.$$

4.2.1 Dimensionless Parameters

To non-dimensionalize the flow governing system (4.1)-(4.4), we use the following dimensionless parameters

$$U = \frac{u}{u_o}, \quad V = \frac{v}{u_o}, \quad W = \frac{Lw}{u_o}, \quad T = \frac{u_o t}{L}, \quad X = \frac{x}{L}, \quad Y = \frac{y}{L}, \quad P = \frac{p}{\rho u_o^2}. \quad (4.5)$$

4.3 Conversion of Dimensional form into Dimensionless Form

To convert governing equations (4.1)-(4.4) into the dimensionless partial differential form, different derivatives are required which have been computed in the upcoming part of this sub-section.

- $X = \frac{x}{L} \Rightarrow \frac{\partial X}{\partial x} = \frac{1}{L}$
- $Y = \frac{y}{L} \Rightarrow \frac{\partial Y}{\partial y} = \frac{1}{L}$
- $U = \frac{u}{u_o} \Rightarrow u = u_o U$
- $V = \frac{v}{u_o} \Rightarrow v = u_o V$
- $W = \frac{Lw}{u_o} \Rightarrow w = \frac{u_o W}{L}$
- $T = \frac{u_o t}{L} \Rightarrow \frac{\partial T}{\partial t} = \frac{u_o}{L}$
- $\frac{\partial u}{\partial t} = \frac{\partial u}{\partial T} \frac{\partial T}{\partial t} = \frac{\partial}{\partial T}(u) \frac{\partial}{\partial t}(T) = \frac{\partial}{\partial T}(u_o U) \frac{u_o}{L} = u_o \frac{\partial U}{\partial T} \frac{u_o}{L} = \frac{u_o^2}{L} \frac{\partial U}{\partial T}$
- $\frac{\partial u}{\partial x} = \frac{\partial u}{\partial X} \frac{\partial X}{\partial x} = \frac{\partial}{\partial X}(u) \frac{1}{L} = \frac{\partial}{\partial X}(u_o U) \frac{1}{L} = \frac{u_o}{L} \frac{\partial U}{\partial X}$

$$\begin{aligned}
& \bullet \frac{\partial u}{\partial y} = \frac{\partial u}{\partial Y} \frac{\partial Y}{\partial y} = \frac{\partial}{\partial Y}(u) \frac{1}{L} = \frac{\partial}{\partial Y}(u_o U) \frac{1}{L} = \frac{u_o}{L} \frac{\partial U}{\partial Y} \\
& \bullet \frac{\partial v}{\partial y} = \frac{\partial v}{\partial Y} \frac{\partial Y}{\partial y} = \frac{\partial}{\partial Y}(v) \frac{1}{L} = \frac{\partial}{\partial Y}(u_o V) \frac{1}{L} = \frac{u_o}{L} \frac{\partial V}{\partial Y} \\
& \bullet u \frac{\partial u}{\partial x} = u_o U \frac{u_o}{L} \frac{\partial U}{\partial X} = \frac{u_o^2}{L} U \frac{\partial U}{\partial X} \\
& \bullet v \frac{\partial u}{\partial y} = u_o V \frac{u_o}{L} \frac{\partial U}{\partial Y} = \frac{u_o^2}{L} V \frac{\partial U}{\partial Y} \\
& \bullet \frac{\partial v}{\partial t} = \frac{\partial v}{\partial T} \frac{\partial T}{\partial t} = \frac{\partial}{\partial T}(v) \frac{\partial}{\partial t}(T) = \frac{\partial}{\partial T}(u_o V) \frac{u_o}{L} = u_o \frac{\partial V}{\partial T} \frac{u_o}{L} = \frac{u_o^2}{L} \frac{\partial V}{\partial T} \\
& \bullet \frac{\partial v}{\partial x} = \frac{\partial v}{\partial X} \frac{\partial X}{\partial x} = \frac{\partial}{\partial X}(v) \frac{1}{L} = \frac{\partial}{\partial X}(u_o V) \frac{1}{L} = \frac{u_o}{L} \frac{\partial V}{\partial X} = u_o U \frac{u_o}{L} \frac{\partial V}{\partial X} = \frac{u_o^2}{L} U \frac{\partial V}{\partial X} \\
& \bullet v \frac{\partial v}{\partial y} = u_o V \frac{u_o}{L} \frac{\partial V}{\partial Y} = \frac{u_o^2}{L} V \frac{\partial V}{\partial Y} \\
& \bullet \frac{\partial w}{\partial t} = \frac{\partial w}{\partial T} \frac{\partial T}{\partial t} = \frac{\partial}{\partial T}(w) \frac{\partial}{\partial t}(T) = \frac{\partial}{\partial T}\left(\frac{u_o W}{L}\right) \frac{u_o}{L} = \frac{u_o^2}{L^2} \frac{\partial W}{\partial T} = \frac{u_o^2}{L^2} \frac{\partial W}{\partial T} \\
& \bullet \frac{\partial w}{\partial x} = \frac{\partial w}{\partial X} \frac{\partial X}{\partial x} = \frac{\partial}{\partial X}(w) \frac{1}{L} = \frac{\partial}{\partial X}\left(\frac{u_o W}{L}\right) \frac{1}{L} = \frac{u_o}{L^2} \frac{\partial W}{\partial X} \\
& \bullet \frac{\partial w}{\partial y} = \frac{\partial w}{\partial Y} \frac{\partial Y}{\partial y} = \frac{\partial}{\partial Y}(w) \frac{1}{L} = \frac{\partial}{\partial Y}\left(\frac{u_o W}{L}\right) \frac{1}{L} = \frac{u_o}{L^2} \frac{\partial W}{\partial Y} \\
& \bullet u \frac{\partial w}{\partial x} = u_o U \frac{u_o}{L^2} \frac{\partial W}{\partial X} = \frac{u_o^2}{L^2} U \frac{\partial W}{\partial X} \\
& \bullet v \frac{\partial w}{\partial y} = u_o V \frac{u_o}{L^2} \frac{\partial W}{\partial Y} = \frac{u_o^2}{L^2} V \frac{\partial W}{\partial Y} \\
& \bullet \frac{\partial^2 w}{\partial x^2} = \frac{\partial}{\partial x} \left(\frac{\partial w}{\partial x} \right) = \frac{\partial}{\partial x} \left(\frac{u_o}{L^2} \frac{\partial W}{\partial X} \right) = \frac{\partial}{\partial X} \frac{\partial X}{\partial x} \left(\frac{u_o}{L^2} \frac{\partial W}{\partial X} \right) \\
& = \frac{\partial}{\partial X} \frac{1}{L} \left(\frac{u_o}{L^2} \frac{\partial W}{\partial X} \right) = \frac{u_o}{L^3} \frac{\partial^2 W}{\partial X^2} \\
& \bullet \frac{\partial^2 w}{\partial y^2} = \frac{\partial}{\partial y} \left(\frac{\partial w}{\partial y} \right) = \frac{\partial}{\partial y} \left(\frac{u_o}{L^2} \frac{\partial W}{\partial Y} \right) = \frac{\partial}{\partial Y} \frac{\partial Y}{\partial y} \left(\frac{u_o}{L^2} \frac{\partial W}{\partial Y} \right) \\
& = \frac{\partial}{\partial Y} \frac{1}{L} \left(\frac{u_o}{L^2} \frac{\partial W}{\partial Y} \right) = \frac{u_o}{L^3} \frac{\partial^2 W}{\partial Y^2}
\end{aligned}$$

$$\begin{aligned}
\bullet \quad uB_xB_y - vB_x^2 &= (u_oU)[(\mu_oH_o + M_o)(-\tau M_o w)] - (u_oV)(\mu_oH_o + M_o)^2 \\
&= (u_oUw)[- \tau M_o(\mu_oH_o + M_o)] - (u_oV)(\mu_oH_o + M_o)^2 \\
&= \left(\frac{Wu_o^2}{L}U\right)[- \tau M_o(\mu_oH_o + M_o)] - (u_oV)(\mu_oH_o + M_o)^2 \\
&= \frac{u_o^2}{L}UW[- \tau M_o(\mu_oH_o + M_o)] - u_o(\mu_oH_o + M_o)^2V
\end{aligned}$$

Now, the dimensionless form of the continuity equation (4.1) can be obtained as follows,

$$\begin{aligned}
\frac{\partial u}{\partial x} + \frac{\partial v}{\partial y} &= 0, \\
\frac{u_o}{L} \frac{\partial U}{\partial X} + \frac{u_o}{L} \frac{\partial V}{\partial Y} &= 0, \\
\frac{u_o}{L} \left(\frac{\partial U}{\partial X} + \frac{\partial V}{\partial Y} \right) &= 0,
\end{aligned}$$

As $\frac{u_o}{L} \neq 0$ but,

$$\frac{\partial U}{\partial X} + \frac{\partial V}{\partial Y} = 0. \quad (4.6)$$

The dimensionless form of the u -momentum equation (4.2) can be obtained as follows,

$$\frac{\partial u}{\partial t} + u \frac{\partial u}{\partial x} + v \frac{\partial u}{\partial y} = -\frac{1}{\rho} \frac{\partial p}{\partial x} + \frac{1}{\rho} (\mu + k) \left(\frac{\partial^2 u}{\partial x^2} + \frac{\partial^2 u}{\partial y^2} \right) + \frac{k}{\rho} \frac{\partial w}{\partial y} + vB_xB_y - uB_y^2,$$

$$\begin{aligned}
\frac{u_o^2}{L} \frac{\partial U}{\partial T} + \frac{u_o^2}{L} U \frac{\partial U}{\partial X} + \frac{u_o^2}{L} V \frac{\partial U}{\partial Y} &= -\frac{1}{\rho} \frac{\partial p}{\partial x} + \frac{1}{\rho} (\mu + k) \left(\frac{u_o}{L^2} \frac{\partial^2 U}{\partial X^2} + \frac{u_o}{L^2} \frac{\partial^2 U}{\partial Y^2} \right) \\
+ \frac{k}{\rho} \frac{u_o}{L^2} \frac{\partial W}{\partial Y} + \frac{u_o^2}{L} VW[- \tau M_o(\mu_oH_o + M_o)] &- \tau^2 u_o M_o^2 \frac{u_o^2}{L^2} UW^2,
\end{aligned}$$

$$\begin{aligned}
\frac{u_o^2}{L} \left[\frac{\partial U}{\partial T} + U \frac{\partial U}{\partial X} + V \frac{\partial U}{\partial Y} \right] &= -\frac{1}{\rho} \frac{\partial p}{\partial x} + \frac{\mu}{\rho} \left(1 + \frac{k}{\mu} \right) \frac{u_o}{L^2} \left(\frac{\partial^2 U}{\partial X^2} + \frac{\partial^2 U}{\partial Y^2} \right) \\
+ \frac{k}{\rho} \frac{u_o}{L^2} \frac{\partial W}{\partial Y} + \frac{u_o^2}{L} VW[\tau M_o(\mu_oH_o + M_o)] &- \tau^2 u_o M_o^2 \frac{u_o^2}{L^2} UW^2,
\end{aligned}$$

$$\begin{aligned} \frac{\partial U}{\partial T} + U \frac{\partial U}{\partial X} + V \frac{\partial U}{\partial Y} &= -\frac{L}{u_o^2} \frac{1}{\rho} \frac{\partial p}{\partial x} + \frac{L\mu}{\rho u_o^2} (1+K) \frac{u_o}{L^2} \left(\frac{\partial^2 U}{\partial X^2} + \frac{\partial^2 U}{\partial Y^2} \right) \\ &+ \frac{Lk u_o}{\rho u_o^2 L^2} \frac{\partial W}{\partial Y} + \frac{L}{u_o^2} \frac{u_o^2}{L} VW [-\tau M_o (\mu_o H_o + M_o)] - \\ &\frac{L}{u_o^2} \tau^2 u_o M_o^2 \frac{u_o^2}{L^2} UW^2, \end{aligned}$$

$$\begin{aligned} \frac{\partial U}{\partial T} + U \frac{\partial U}{\partial X} + V \frac{\partial U}{\partial Y} &= -\frac{L}{u_o^2} \frac{1}{\rho} \frac{\partial}{\partial X} \frac{\partial X}{\partial x} (p) + \frac{\mu}{L \rho u_o} (1+K) \left(\frac{\partial^2 U}{\partial X^2} + \frac{\partial^2 U}{\partial Y^2} \right) \\ &+ \frac{\frac{k}{\rho u_o L}}{\mu} \frac{\partial W}{\partial Y} + VW [-\tau M_o (\mu_o H_o + M_o)] - \tau^2 \frac{u_o}{L} M_o^2 UW^2, \end{aligned}$$

$$\begin{aligned} \frac{\partial U}{\partial T} + U \cdot \frac{\partial U}{\partial X} + V \cdot \frac{\partial U}{\partial Y} &= \frac{1}{\frac{\rho L u_o}{\mu}} (1+K) \left(\frac{\partial^2 U}{\partial X^2} + \frac{\partial^2 U}{\partial Y^2} \right) - L \frac{\partial}{\partial X} \frac{1}{L} \left(\frac{p}{\rho u_o^2} \right) \\ &+ \frac{K}{Re} \frac{\partial W}{\partial Y} + VW [-\alpha] - \tau^2 M_o^2 \frac{u_o}{L} UW^2, \end{aligned}$$

$$\begin{aligned} \frac{\partial U}{\partial T} + U \cdot \frac{\partial U}{\partial X} + V \cdot \frac{\partial U}{\partial Y} &= \frac{1}{Re} (1+K) \left(\frac{\partial^2 U}{\partial X^2} + \frac{\partial^2 U}{\partial Y^2} \right) - \frac{\partial P}{\partial X} + \frac{K}{Re} \frac{\partial W}{\partial Y} - \alpha VW - \beta UW^2, \end{aligned} \quad (4.7)$$

Similarly, the dimensionless form of the v -momentum equation (4.3) can be obtained as follows,

$$\begin{aligned} \frac{\partial v}{\partial t} + u \frac{\partial v}{\partial x} + v \frac{\partial v}{\partial y} &= -\frac{1}{\rho} \frac{\partial p}{\partial y} + \frac{1}{\rho} (\mu + k) \\ &\left(\frac{\partial^2 v}{\partial x^2} + \frac{\partial^2 v}{\partial y^2} \right) - \frac{k}{\rho} \frac{\partial w}{\partial x} + u B_x B_y - v B_x^2, \end{aligned}$$

$$\begin{aligned} \frac{u_o^2}{L} \frac{\partial V}{\partial T} + \frac{u_o^2}{L} U \frac{\partial V}{\partial X} + \frac{u_o^2}{L} V \frac{\partial V}{\partial Y} &= -\frac{1}{\rho} \frac{\partial p}{\partial y} + \frac{1}{\rho} (\mu + k) \left(\frac{u_o}{L^2} \frac{\partial^2 V}{\partial X^2} + \frac{u_o}{L^2} \frac{\partial^2 V}{\partial Y^2} \right) \\ &- \frac{k}{\rho L^2} \frac{\partial W}{\partial X} + \frac{u_o^2}{L} UW [-\tau M_o (\mu_o H_o + M_o)] - u_o (\mu_o H_o + M_o)^2 V, \end{aligned}$$

$$\begin{aligned} \frac{u_o^2}{L} \left[\frac{\partial V}{\partial T} + U \frac{\partial V}{\partial X} + V \frac{\partial V}{\partial Y} \right] &= -\frac{1}{\rho} \frac{\partial p}{\partial y} + \frac{\mu}{\rho} (1 + \frac{k}{\mu}) \frac{u_o}{L^2} \left(\frac{\partial^2 V}{\partial X^2} + \frac{\partial^2 V}{\partial Y^2} \right) \\ &- \frac{k}{\rho L^2} \frac{\partial W}{\partial X} + \frac{u_o^2}{L} UW [-\tau M_o (\mu_o H_o + M_o)] - u_o (\mu_o H_o + M_o)^2 V, \end{aligned}$$

$$\begin{aligned} \frac{\partial V}{\partial T} + U \frac{\partial V}{\partial X} + V \frac{\partial V}{\partial Y} &= -\frac{L}{u_o^2} \frac{1}{\rho} \frac{\partial p}{\partial y} + \frac{L}{u_o^2} \frac{\mu}{\rho} (1+K) \frac{u_o}{L^2} \left(\frac{\partial^2 V}{\partial X^2} + \frac{\partial^2 V}{\partial Y^2} \right) \\ &- \frac{L}{u_o^2} \frac{k}{\rho} \frac{u_o}{L^2} \frac{\partial W}{\partial X} + \frac{L}{u_o^2} \frac{u_o^2}{L} UW [-\tau M_o (\mu_o H_o + M_o)] - \frac{L}{u_o^2} u_o (\mu_o H_o + M_o)^2 V, \end{aligned}$$

$$\begin{aligned} \frac{\partial V}{\partial T} + U \frac{\partial V}{\partial X} + V \frac{\partial V}{\partial Y} + \frac{L}{u_o^2} \frac{1}{\rho} \frac{\partial}{\partial Y} \frac{\partial Y}{\partial y} (p) &= \frac{\mu}{\rho L u_o} (1+K) \left(\frac{\partial^2 V}{\partial X^2} + \frac{\partial^2 V}{\partial Y^2} \right) \\ &- \frac{k}{\rho L u_o} \frac{\partial W}{\partial X} + UW [-\tau M_o (\mu_o H_o + M_o)] - \frac{L}{u_o} (\mu_o H_o + M_o)^2 V, \end{aligned}$$

$$\begin{aligned} \frac{\partial V}{\partial T} + U \frac{\partial V}{\partial X} + V \frac{\partial V}{\partial Y} &= -L \frac{\partial}{\partial Y} \frac{1}{L} \left(\frac{p}{\rho u_o^2} \right) + \frac{1}{\rho L u_o} (1+K) \left(\frac{\partial^2 V}{\partial X^2} + \frac{\partial^2 V}{\partial Y^2} \right) \\ &- \frac{\frac{k}{\mu}}{\rho L u_o} \frac{\partial W}{\partial X} + UW [-\alpha] - \frac{L}{u_o} \frac{\tau M_o}{\tau M_o} (\mu_o H_o + M_o) (\mu_o H_o + M_o) V, \end{aligned}$$

$$\begin{aligned} \frac{\partial V}{\partial T} + U \frac{\partial V}{\partial X} + V \frac{\partial V}{\partial Y} + \frac{\partial P}{\partial Y} &= \frac{1}{Re} (1+K) \left(\frac{\partial^2 V}{\partial X^2} + \frac{\partial^2 V}{\partial Y^2} \right) - \frac{K}{Re} \frac{\partial W}{\partial X} \\ &- \alpha UW - \alpha \left(\frac{L}{u_o \tau M_o} \right) (\mu_o H_o + M_o) \frac{\tau M_o}{\tau M_o} V, \end{aligned}$$

$$\begin{aligned} \frac{\partial V}{\partial T} + U \frac{\partial V}{\partial X} + V \frac{\partial V}{\partial Y} + \frac{\partial P}{\partial Y} &= \frac{1}{Re} (1+K) \left(\frac{\partial^2 V}{\partial X^2} + \frac{\partial^2 V}{\partial Y^2} \right) \\ &- \frac{K}{Re} \frac{\partial W}{\partial X} - \alpha UW - \left(\frac{L}{u_o \tau^2 M_o^2} \right) \alpha^2 V, \end{aligned}$$

$$\begin{aligned} \frac{\partial V}{\partial T} + U \frac{\partial V}{\partial X} + V \frac{\partial V}{\partial Y} + \frac{\partial P}{\partial Y} &= \\ &\frac{1}{Re} (1+K) \left(\frac{\partial^2 V}{\partial X^2} + \frac{\partial^2 V}{\partial Y^2} \right) - \frac{K}{Re} \frac{\partial W}{\partial X} - \alpha UW - \left(\frac{\alpha^2}{\beta} \right) V, \end{aligned} \quad (4.8)$$

Now, the dimensionless form of the micromagnetorotational model (4.4) can be obtained as follows,

$$\frac{\partial w}{\partial t} + u \frac{\partial w}{\partial x} + v \frac{\partial w}{\partial y} = \frac{\gamma^*}{\rho j} \left(\frac{\partial^2 w}{\partial x^2} + \frac{\partial^2 w}{\partial y^2} \right) + \frac{2k}{\rho j} \left(\frac{\partial v}{\partial x} - \frac{\partial u}{\partial y} - 2w \right),$$

$$\begin{aligned}
& \frac{u_o^2}{L^2} \frac{\partial W}{\partial T} + \frac{u_o^2}{L^2} U \frac{\partial W}{\partial X} + \frac{u_o^2}{L^2} V \frac{\partial W}{\partial Y} \\
& \quad = \frac{\gamma^*}{\rho j} \left(\frac{u_o}{L^3} \frac{\partial^2 W}{\partial X^2} + \frac{u_o}{L^3} \frac{\partial^2 W}{\partial Y^2} \right) + \frac{2k}{\rho j} \left(\frac{u_o}{L} \frac{\partial V}{\partial X} - \frac{u_o}{L} \frac{\partial U}{\partial Y} - 2 \frac{u_o W}{L} \right), \\
& \frac{u_o^2}{L^2} \left[\frac{\partial W}{\partial T} + U \frac{\partial W}{\partial X} + V \frac{\partial W}{\partial Y} \right] \\
& \quad = \frac{\gamma^*}{\rho j} \left(\frac{u_o}{L^3} \left(\frac{\partial^2 W}{\partial X^2} + \frac{\partial^2 W}{\partial Y^2} \right) \right) + \frac{2k}{\rho j} \left(\frac{u_o}{L} \left(\frac{\partial V}{\partial X} - \frac{\partial U}{\partial Y} \right) - 2 \frac{u_o W}{L} \right), \\
& \frac{\partial W}{\partial T} + U \frac{\partial W}{\partial X} + V \frac{\partial W}{\partial Y} \\
& \quad = \frac{L^2 \gamma^* u_o}{u_o^2 \rho j L^3} \left(\frac{\partial^2 W}{\partial X^2} + \frac{\partial^2 W}{\partial Y^2} \right) + \frac{2k}{\rho j} \left(\frac{L^2 u_o}{u_o^2 L} \left(\frac{\partial V}{\partial X} - \frac{\partial U}{\partial Y} \right) - 2 \frac{u_o W L^2}{L u_o^2} \right), \\
& \frac{\partial W}{\partial T} + U \frac{\partial W}{\partial X} + V \frac{\partial W}{\partial Y} = \frac{\gamma^*}{\rho j} \frac{1}{u_o L} \left(\frac{\partial^2 W}{\partial X^2} + \frac{\partial^2 W}{\partial Y^2} \right) + \frac{2k}{\rho j} \left(\frac{L}{u_o} \left(\frac{\partial V}{\partial X} - \frac{\partial U}{\partial Y} \right) - 2 \frac{W L}{u_o} \right), \\
& \frac{\partial W}{\partial T} + U \frac{\partial W}{\partial X} + V \frac{\partial W}{\partial Y} = \frac{\gamma^*}{\rho j} \frac{1}{u_o L} \left(\frac{\partial^2 W}{\partial X^2} + \frac{\partial^2 W}{\partial Y^2} \right) + \frac{2k L}{\rho j u_o} \left(\frac{\partial V}{\partial X} - \frac{\partial U}{\partial Y} - 2W \right), \\
& \frac{\partial W}{\partial T} + U \frac{\partial W}{\partial X} + V \frac{\partial W}{\partial Y} = \frac{\gamma^*}{\frac{\rho u_o L}{\mu} j \mu} \left(\frac{\partial^2 W}{\partial X^2} + \frac{\partial^2 W}{\partial Y^2} \right) + \frac{2k L \cdot L}{\rho u_o j \cdot L} \left(\frac{\partial V}{\partial X} - \frac{\partial U}{\partial Y} - 2W \right), \\
& \frac{\partial W}{\partial T} + U \frac{\partial W}{\partial X} + V \frac{\partial W}{\partial Y} - \frac{\gamma^*}{Re \mu j} \left(\frac{\partial^2 W}{\partial X^2} + \frac{\partial^2 W}{\partial Y^2} \right) + \frac{2k L^2}{\frac{\rho u_o L}{\mu} j \mu} \left(\frac{\partial V}{\partial X} - \frac{\partial U}{\partial Y} - 2W \right), \\
& \frac{\partial W}{\partial T} + U \frac{\partial W}{\partial X} + V \frac{\partial W}{\partial Y} - \frac{K_m}{Re} \left(\frac{\partial^2 W}{\partial X^2} + \frac{\partial^2 W}{\partial Y^2} \right) + \frac{2k}{\frac{Re}{L^2} j \mu} \left(\frac{\partial V}{\partial X} - \frac{\partial U}{\partial Y} - 2W \right), \\
& \frac{\partial W}{\partial T} + U \frac{\partial W}{\partial X} + V \frac{\partial W}{\partial Y} - \frac{1}{Re} \left(1 + \frac{K}{2} \right) \left(\frac{\partial^2 W}{\partial X^2} + \frac{\partial^2 W}{\partial Y^2} \right) = \left(\frac{2K}{E_r Re} \right) \left(\frac{\partial V}{\partial X} - \frac{\partial U}{\partial Y} - 2W \right), \tag{4.9}
\end{aligned}$$

4.4 Dimensionless Governing Equations

The set of transformed dimensionless equations can be written as

$$\frac{\partial U}{\partial X} + \frac{\partial V}{\partial Y} = 0. \tag{4.10}$$

$$\begin{aligned}
& \frac{\partial U}{\partial T} + U \frac{\partial U}{\partial X} + V \frac{\partial U}{\partial Y} + \frac{\partial P}{\partial X} = \frac{1}{Re} (1 + K) \left(\frac{\partial^2 U}{\partial X^2} + \frac{\partial^2 U}{\partial Y^2} \right) + \frac{K}{Re} \frac{\partial W}{\partial Y} \\
& \quad - \alpha V W - \beta U W^2. \tag{4.11}
\end{aligned}$$

$$\begin{aligned} \frac{\partial V}{\partial T} + U \frac{\partial V}{\partial X} + V \frac{\partial V}{\partial Y} + \frac{\partial P}{\partial Y} = \frac{1}{Re} (1 + K) \left(\frac{\partial^2 V}{\partial X^2} + \frac{\partial^2 V}{\partial Y^2} \right) - \frac{K}{Re} \frac{\partial W}{\partial X} \\ - \alpha U W - \left(\frac{\alpha^2}{\beta} \right) V. \end{aligned} \quad (4.12)$$

$$\frac{\partial W}{\partial T} + U \frac{\partial W}{\partial X} + V \frac{\partial W}{\partial Y} - \frac{1}{Re} \left(\left(1 + \frac{K}{2} \right) \left(\frac{\partial^2 W}{\partial X^2} + \frac{\partial^2 W}{\partial Y^2} \right) \right) = \frac{2K}{E_r} \left(\frac{\partial V}{\partial X} - \frac{\partial U}{\partial Y} - 2W \right). \quad (4.13)$$

In (4.10) to (4.13), the nondimensional parameters Re represent Reynolds number, K is Micropolar flow, γ^* is the spin gradient viscosity and K_m is micro-inertial parameter respectively, defined by

$$\begin{aligned} Re = \frac{\rho L u_o}{\mu}, \quad K = \frac{k}{\mu}, \quad K_m = \frac{\gamma^*}{\mu j}, \quad E_r = \frac{j}{L^2}, \\ \gamma^* = \mu \left(1 + \frac{K}{2} \right) j, \quad \alpha = \tau M_o (\mu_o H_o + M_o), \quad \beta = \frac{u_o \tau^2 M_o^2}{L}. \end{aligned} \quad (4.14)$$

The associated dimensionless boundary conditions are as follows:

- At inlet (A-F):

$$U = (H - Y)(Y - \frac{1}{2}) / \sqrt{(H - 0.5)/2}, \quad V = 0, \quad W = 0$$

- At the walls (A-B, B-C, C-D and E-F):

$$U = 0, \quad V = 0, \quad W = 0.$$

- At outlet (E-D):

$$\frac{\partial U}{\partial X} = 0, \quad \frac{\partial V}{\partial X} = 0, \quad \frac{\partial W}{\partial X} = 0.$$

4.5 Weak formulation/Variational form of the problem

Weak formulation is a variational method that multiplies the dependent variables by an appropriate test function and then integrates the result over the entire

computational domain to convert differential equations into integral form. In this case, the solution spaces U , V , W , and P are defined on the continuously varying infinite dimensional space Ω ; in actuality, it is impossible to achieve the solution in such a large space.

Finding some appropriate spaces to obtain functions with finite parameters or properties is the main goal. In order to find an approximate solution using the weak formulation, we must first define a few unique functions that we will refer to as test functions for the residuals.

Assume that \bar{W} and Q represent the infinite-dimensional test space where

$$\bar{W} = [H_1(\Omega), H_1(\Omega), H_1(\Omega)] \text{ and } Q = L_2(\Omega).$$

The corresponding test functions, \tilde{U} , \tilde{V} , \tilde{W} and q should be such that \tilde{U} , \tilde{V} , $\tilde{W} \in \bar{W}$ and $q \in Q$. The test functions \tilde{U} , \tilde{V} , $\tilde{W} \in \bar{W}$ multiplies the momentum and micromagnetorotational equation components in the variational formulation. The weak formulation of the strong form of governing PDEs from Eqs. (4.10) to (4.13) is written below:

The weak form for u -component is as follows:

$$\begin{aligned} \frac{\partial U}{\partial T} + U \frac{\partial U}{\partial X} + V \frac{\partial U}{\partial Y} = & -\frac{\partial P}{\partial X} + \frac{1}{Re}(1 + K) \left(\frac{\partial^2 U}{\partial X^2} + \frac{\partial^2 U}{\partial Y^2} \right) \\ & + \frac{K}{Re} \frac{\partial W}{\partial Y} - \alpha VW - \beta UW^2 \end{aligned}$$

After some manipulations we arrive at:

$$\begin{aligned} \frac{\partial U}{\partial T} \tilde{U} + \left[\left(U \frac{\partial U}{\partial X} \right) + \left(V \frac{\partial U}{\partial Y} \right) \right] \tilde{U} - q \frac{\partial}{\partial X} (U \tilde{U}) \\ + q U \frac{\partial \tilde{U}}{\partial X} = & -\frac{\partial}{\partial X} (P \tilde{U}) + P \frac{\partial \tilde{U}}{\partial X} + \frac{1}{Re}(1 + K) \left\{ \frac{\partial^2 U}{\partial X^2} + \frac{\partial^2 U}{\partial Y^2} \right\} \tilde{U} \\ + \frac{K}{Re} \frac{\partial}{\partial Y} (W \tilde{U}) - \frac{K}{Re} W \frac{\partial \tilde{U}}{\partial Y} - \frac{\alpha}{2} (VW + VW) \tilde{U} \frac{\beta}{2} (UW^2 + UW^2) \tilde{U} \end{aligned}$$

$$\begin{aligned}
& \int_{\Omega^n} \frac{\partial U}{\partial T} \tilde{U} d\Omega + \int_{\Omega^n} \left[\left(U \frac{\partial U}{\partial X} \right) + \left(V \frac{\partial U}{\partial Y} \right) \right] \tilde{U} d\Omega - q \int_{\Omega^n} \frac{\partial}{\partial X} (U \tilde{U}) d\Omega \\
& + q \int_{\Omega^n} U \frac{\partial \tilde{U}}{\partial X} d\Omega = - \int_{\Omega^n} \frac{\partial}{\partial X} (P \tilde{U}) d\Omega + P \int_{\Omega^n} \frac{\partial \tilde{U}}{\partial X} d\Omega + \\
& \frac{1}{Re} (1 + K) \int_{\Omega^n} \left\{ \frac{\partial^2 U}{\partial X^2} + \frac{\partial^2 U}{\partial Y^2} \right\} \tilde{U} d\Omega \tag{4.15} \\
& + \frac{K}{Re} \int_{\Omega^n} \frac{\partial}{\partial Y} (W \tilde{U}) d\Omega - \frac{K}{Re} \int_{\Omega^n} W \frac{\partial \tilde{U}}{\partial Y} d\Omega - \frac{\alpha}{2} \int_{\Omega^n} (VW + VW) \tilde{U} d\Omega \\
& - \frac{\beta}{2} \int_{\Omega^n} (UW^2 + UW^2) \tilde{U} d\Omega
\end{aligned}$$

$$\begin{aligned}
\text{As } & \int_{\Omega^n} \frac{\partial U}{\partial T} \tilde{U} d\Omega + \int_{\Omega^n} \left[U \frac{\partial U}{\partial X} + V \frac{\partial U}{\partial Y} \right] \tilde{U} d\Omega \\
& = \int_{\Omega^n} \frac{(U^{n+1} - U^n)}{\delta t} \tilde{U} d\Omega + \int_{\Omega^n} \left[U \frac{\partial U}{\partial X} + V \frac{\partial U}{\partial Y} \right] \tilde{U} d\Omega \\
& = \frac{1}{\delta t} \int_{\Omega^n} U^{n+1} \tilde{U} d\Omega - \frac{1}{\delta t} \int_{\Omega^n} U^n \tilde{U} d\Omega + \int_{\Omega^n} \left[U \frac{\partial U}{\partial X} + V \frac{\partial U}{\partial Y} \right] \tilde{U} d\Omega \\
& = \frac{1}{\delta t} \int_{\Omega^n} U^{n+1} \tilde{U} d\Omega - \frac{1}{\delta t} \left(U^n \circ X^n \right) \tilde{U} d\Omega
\end{aligned}$$

$$\begin{aligned}
& \frac{1}{\delta t} \int_{\Omega^n} U^{n+1} \tilde{U} d\Omega - \frac{1}{\delta t} \left(U^n \circ X^n \right) \tilde{U} d\Omega - q \int_{\Omega^n} \frac{\partial}{\partial X} (U \tilde{U}) d\Omega + q \int_{\Omega^n} U \frac{\partial \tilde{U}}{\partial X} d\Omega \\
& = - \int_{\Omega^n} \frac{\partial}{\partial X} (P \tilde{U}) d\Omega + P \int_{\Omega^n} \frac{\partial \tilde{U}}{\partial X} d\Omega + \\
& \frac{1}{Re} (1 + K) \int_{\Omega^n} \left\{ \frac{\partial^2 U}{\partial X^2} + \frac{\partial^2 U}{\partial Y^2} \right\} \tilde{U} d\Omega \\
& + \frac{K}{Re} \int_{\Omega^n} \frac{\partial}{\partial Y} (W \tilde{U}) d\Omega - \\
& \frac{K}{Re} \int_{\Omega^n} W \frac{\partial \tilde{U}}{\partial Y} d\Omega - \\
& \frac{\alpha}{2} \int_{\Omega^n} (VW + VW) \tilde{U} d\Omega - \\
& \frac{\beta}{2} \int_{\Omega^n} (UW^2 + UW^2) \tilde{U} d\Omega
\end{aligned}$$

$$\begin{aligned}
& \frac{1}{\delta t} \int_{\Omega^n} U^{n+1} \tilde{U} d\Omega - \frac{1}{\delta t} \left(U^n \circ X^n \right) \tilde{U} d\Omega - q \int_{\Omega^n} \frac{\partial}{\partial X} (U \tilde{U}) d\Omega \\
& + q \int_{\Omega^n} U \frac{\partial \tilde{U}}{\partial X} d\Omega = \int_{\Omega^n} \frac{\partial}{\partial X} (P \tilde{U}) d\Omega + P \int_{\Omega^n} \frac{\partial \tilde{U}}{\partial X} d\Omega + \\
& \frac{1}{Re} (1 + K) \int_{\Omega^n} \left\{ \frac{\partial^2 U}{\partial X^2} + \frac{\partial^2 U}{\partial Y^2} \right\} \tilde{U} d\Omega + \frac{K}{Re} \int_{\Omega^n} \frac{\partial}{\partial Y} (W \tilde{U}) d\Omega - \frac{K}{Re} \int_{\Omega^n} W \frac{\partial \tilde{U}}{\partial Y} d\Omega \\
& - \frac{\alpha}{2} \int_{\Omega^n} (VW + VW) \tilde{U} d\Omega - \frac{\beta}{2} \int_{\Omega^n} (UW^2 + UW^2) \tilde{U} d\Omega
\end{aligned}$$

$$\begin{aligned}
& \frac{1}{\delta t} \int_{\Omega^n} U^{n+1} \tilde{U} d\Omega - \frac{1}{\delta t} \left(U^n \circ X^n \right) \tilde{U} d\Omega + q \int_{\Omega^n} U \frac{\partial \tilde{U}}{\partial X} d\Omega \\
& = P \int_{\Omega^n} \frac{\partial \tilde{U}}{\partial X} d\Omega + \frac{1}{Re} (1 + K) \int_{\Omega^n} \left\{ \frac{\partial^2 U}{\partial X^2} + \frac{\partial^2 U}{\partial Y^2} \right\} \tilde{U} d\Omega - \frac{K}{Re} \int_{\Omega^n} W \frac{\partial \tilde{U}}{\partial Y} d\Omega \quad (4.16) \\
& - \frac{\alpha}{2} \int_{\Omega^n} (VW + VW) \tilde{U} d\Omega - \frac{\beta}{2} \int_{\Omega^n} (UW^2 + UW^2) \tilde{U} d\Omega
\end{aligned}$$

Using Green's theorem for Laplacian term as

$$\int_{\Omega} \psi \Delta \phi d\Omega = - \int_{\Omega} \nabla \phi \nabla \psi d\Omega + \int_{\Omega} \psi (\nabla \phi n) d\Gamma$$

$$\text{Here, } \psi = \tilde{U}, \Delta \phi = \frac{\partial^2 U}{\partial X^2}, \Delta \phi = \frac{\partial^2 U}{\partial Y^2}, \nabla \phi = \frac{\partial U}{\partial X}, \nabla \phi = \frac{\partial U}{\partial Y}, \nabla \psi = \frac{\partial \tilde{U}}{\partial X},$$

$$\nabla \psi = \frac{\partial \tilde{U}}{\partial Y}$$

$$\text{As } \nabla \phi n = \frac{\partial \phi}{\partial n} = n_x \frac{\partial \phi}{\partial X} + n_y \frac{\partial \phi}{\partial Y} \quad (\phi = U)$$

So,

$$\begin{aligned}
& \frac{1}{Re} (1 + K) \int_{\Omega^n} \left\{ \frac{\partial^2 U}{\partial X^2} + \frac{\partial^2 U}{\partial Y^2} \right\} \tilde{U} d\Omega = \\
& \frac{1}{Re} (1 + K) \left\{ - \int_{\Omega^n} \frac{\partial U}{\partial X} \frac{\partial \tilde{U}}{\partial X} d\Omega + \oint_{\Gamma} \tilde{U} \left(n_x \frac{\partial U}{\partial X} \right) d\Gamma \right. \\
& \left. - \int_{\Omega^n} \frac{\partial U}{\partial Y} \frac{\partial \tilde{U}}{\partial Y} d\Omega + \oint_{\Gamma} \tilde{U} \left(n_y \frac{\partial U}{\partial Y} \right) d\Gamma \right\}
\end{aligned}$$

Now (4.16) becomes as

$$\begin{aligned}
& \frac{1}{\delta t} \int_{\Omega^n} U^{n+1} \tilde{U} d\Omega - \frac{1}{\delta t} \left(U^n \circ X^n \right) \tilde{U} d\Omega + q \int_{\Omega^n} U \frac{\partial \tilde{U}}{\partial X} d\Omega \\
& = P \int_{\Omega^n} \frac{\partial \tilde{U}}{\partial X} d\Omega + \frac{1}{Re} (1 + K) \left\{ \int_{\Omega^n} \frac{\partial U}{\partial X} \frac{\partial \tilde{U}}{\partial X} d\Omega + \oint_{\Gamma} \tilde{U} \left(n_x \frac{\partial U}{\partial X} \right) d\Gamma \right. \\
& \quad \left. - \int_{\Omega} \frac{\partial U}{\partial Y} \frac{\partial \tilde{U}}{\partial Y} d\Omega + \oint_{\Gamma} \tilde{U} \left(n_y \frac{\partial U}{\partial Y} \right) d\Gamma \right\} \frac{K}{Re} \int_{\Omega^n} W \frac{\partial \tilde{U}}{\partial Y} d\Omega \\
& \quad - \frac{\alpha}{2} \int_{\Omega^n} (VW + VW) \tilde{U} d\Omega - \frac{\beta}{2} \int_{\Omega^n} (UW^2 + UW^2) \tilde{U} d\Omega
\end{aligned}$$

Taking Domain as current time step value, we have

$$\begin{aligned}
& \frac{1}{\delta t} \int_{\Omega^{n+1}} U^{n+1} \tilde{U} d\Omega - \frac{1}{\delta t} \left(U^n \circ X^n \right) \tilde{U} d\Omega + q \int_{\Omega^{n+1}} U^{n+1} \frac{\partial \tilde{U}}{\partial X^{n+1}} d\Omega \\
& = P^{n+1} \int_{\Omega^{n+1}} \frac{\partial \tilde{U}}{\partial X^{n+1}} d\Omega + \frac{1}{Re} (1 + K) \left\{ \int_{\Omega^{n+1}} \frac{\partial U^{n+1}}{\partial X^{n+1}} \frac{\partial \tilde{U}}{\partial X^{n+1}} d\Omega \right. \\
& \quad \left. + \oint_{\Gamma} \tilde{U} \left(n_x \frac{\partial U^{n+1}}{\partial X^{n+1}} \right) d\Gamma - \int_{\Omega^{n+1}} \frac{\partial U^{n+1}}{\partial Y^{n+1}} \frac{\partial \tilde{U}}{\partial Y^{n+1}} d\Omega + \oint_{\Gamma} \tilde{U} \left(n_y \frac{\partial U^{n+1}}{\partial Y^{n+1}} \right) d\Gamma \right\} \\
& \quad - \frac{K}{Re} \int_{\Omega^{n+1}} W^{n+1} \frac{\partial \tilde{U}}{\partial Y^{n+1}} d\Omega - \frac{\alpha}{2} \int_{\Omega^{n+1}} (VW + VW)^{n+1} \tilde{U} d\Omega + \\
& \quad \frac{\beta}{2} \int_{\Omega^{n+1}} (UW^2 + UW^2)^{n+1} \tilde{U} d\Omega \\
& \frac{1}{\delta t} \int_{\Omega^{n+1}} U^{n+1} \tilde{U} d\Omega - \frac{1}{\delta t} \left(U^n \circ X^n \right) \tilde{U} d\Omega + q \int_{\Omega^{n+1}} U^{n+1} \frac{\partial \tilde{U}}{\partial X^{n+1}} d\Omega \\
& = P^{n+1} \int_{\Omega^{n+1}} \frac{\partial \tilde{U}}{\partial X^{n+1}} d\Omega + \frac{1}{Re} (1 + K) \left\{ - \int_{\Omega^{n+1}} \frac{\partial U^{n+1}}{\partial X^{n+1}} \frac{\partial \tilde{U}}{\partial X^{n+1}} d\Omega \right. \\
& \quad \left. + \oint_{\Gamma} \tilde{U} \left(n_x \frac{\partial U^{n+1}}{\partial X^{n+1}} \right) d\Gamma - \int_{\Omega^{n+1}} \frac{\partial U^{n+1}}{\partial Y^{n+1}} \frac{\partial \tilde{U}}{\partial Y^{n+1}} d\Omega + \oint_{\Gamma} \tilde{U} \left(n_y \frac{\partial U^{n+1}}{\partial Y^{n+1}} \right) d\Gamma \right\} \\
& \quad - \frac{K}{Re} \int_{\Omega^{n+1}} W^{n+1} \frac{\partial \tilde{U}}{\partial Y^{n+1}} d\Omega - \frac{\alpha}{2} \int_{\Omega^{n+1}} (V^{n+1} W^n + V^n W^{n+1}) \tilde{U} d\Omega \\
& \quad - \frac{\beta}{2} \int_{\Omega^{n+1}} (U^{n+1} W^{2n} + U^n W^{2n+2}) \tilde{U} d\Omega
\end{aligned}$$

which is weak form of u -component of momentum equation.

Find $(U, V, W) \in \bar{W}$ and $P \in Q$ such that

$$\begin{aligned}
& \frac{1}{\delta t} \int_{\Omega^{n+1}} U^{n+1} \tilde{U} d\Omega - \frac{1}{\delta t} \left(U^n \circ X^n \right) \tilde{U} d\Omega + q \int_{\Omega^{n+1}} U^{n+1} \frac{\partial \tilde{U}}{\partial X^{n+1}} d\Omega \\
& - P^{n+1} \int_{\Omega^{n+1}} \frac{\partial \tilde{U}}{\partial X^{n+1}} d\Omega - \frac{1}{Re} (1 + K) \left\{ - \int_{\Omega^{n+1}} \frac{\partial U^{n+1}}{\partial X^{n+1}} \frac{\partial \tilde{U}}{\partial X^{n+1}} d\Omega \right. \\
& + \oint_{\Gamma} \tilde{U} \left(n_x \frac{\partial U^{n+1}}{\partial X^{n+1}} \right) d\Gamma - \int_{\Omega^{n+1}} \frac{\partial U^{n+1}}{\partial Y^{n+1}} \frac{\partial \tilde{U}}{\partial Y^{n+1}} d\Omega + \oint_{\Gamma} \tilde{U} \left(n_y \frac{\partial U^{n+1}}{\partial Y^{n+1}} \right) d\Gamma \left. \right\} \quad (4.17) \\
& + \frac{K}{Re} \int_{\Omega^{n+1}} W^{n+1} \frac{\partial \tilde{U}}{\partial Y^{n+1}} d\Omega + \frac{\alpha}{2} \int_{\Omega^{n+1}} (V^{n+1} W^n + V^n W^{n+1}) \tilde{U} d\Omega \\
& + \frac{\beta}{2} \int_{\Omega^{n+1}} (U^{n+1} W^{2n} + U^n W^{2n+2}) \tilde{U} d\Omega = 0.
\end{aligned}$$

$$\begin{aligned}
& \frac{1}{\delta t} \int_{\Omega^{n+1}} V^{n+1} \tilde{V} d\Omega - \frac{1}{\delta t} \left(V^n \circ Y^n \right) \tilde{V} d\Omega + q \int_{\Omega^{n+1}} V^{n+1} \frac{\partial \tilde{V}}{\partial Y^{n+1}} d\Omega \\
& - P^{n+1} \int_{\Omega^{n+1}} \frac{\partial \tilde{V}}{\partial Y^{n+1}} d\Omega - \frac{1}{Re} (1 + K) \left\{ - \int_{\Omega^{n+1}} \frac{\partial V^{n+1}}{\partial X^{n+1}} \frac{\partial \tilde{V}}{\partial X^{n+1}} d\Omega \right. \\
& + \oint_{\Gamma} \tilde{V} \left(n_x \frac{\partial V^{n+1}}{\partial X^{n+1}} \right) d\Gamma - \int_{\Omega^{n+1}} \frac{\partial V^{n+1}}{\partial Y^{n+1}} \frac{\partial \tilde{V}}{\partial Y^{n+1}} d\Omega \\
& + \oint_{\Gamma} \tilde{V} \left(n_y \frac{\partial V^{n+1}}{\partial Y^{n+1}} \right) d\Gamma \left. \right\} - \frac{K}{Re} \int_{\Omega^{n+1}} W^{n+1} \frac{\partial \tilde{V}}{\partial X^{n+1}} d\Omega \\
& + \frac{\alpha}{2} \int_{\Omega^{n+1}} (U^{n+1} W^n + U^n W^{n+1}) \tilde{V} d\Omega + \left(\frac{\alpha^2}{\beta} \right) \int_{\Omega^{n+1}} V^{n+1} \tilde{V} d\Omega = 0. \quad (4.18)
\end{aligned}$$

$$\begin{aligned}
& \frac{1}{\delta t} \int_{\Omega^{n+1}} W^{n+1} \tilde{W} d\Omega - \frac{1}{\delta t} \left(W^n \circ X^n \right) \tilde{W} d\Omega \\
& - \frac{1}{Re} \left(1 + \frac{K}{2} \right) \left\{ - \int_{\Omega^{n+1}} \frac{\partial W^{n+1}}{\partial X^{n+1}} \frac{\partial \tilde{W}}{\partial X^{n+1}} d\Omega \right. \\
& + \oint_{\Gamma} \tilde{W} \left(n_x \frac{\partial W^{n+1}}{\partial X^{n+1}} \right) d\Gamma - \int_{\Omega^{n+1}} \frac{\partial W^{n+1}}{\partial Y^{n+1}} \frac{\partial \tilde{W}}{\partial Y^{n+1}} d\Omega \\
& + \oint_{\Gamma} \tilde{W} \left(n_y \frac{\partial W^{n+1}}{\partial Y^{n+1}} \right) d\Gamma \left. \right\} \\
& - \frac{2K}{Re E_r} \int_{\Omega^{n+1}} \left(- V^{n+1} \frac{\partial \tilde{W}}{\partial X^{n+1}} + U^{n+1} \frac{\partial \tilde{W}}{\partial Y^{n+1}} - 2W^{n+1} \tilde{W} \right) d\Omega = 0. \quad (4.19)
\end{aligned}$$

for all $\tilde{U}, \tilde{V}, \tilde{W} \in \bar{W}$ and $P \in Q$.

In the Galerkin discretization method, the infinite-dimensional test and trial spaces are approximated by finite-dimensional subspaces. The trial space is comprised of a finite collection of basis functions that approximate the solution space, while the test space is made up of a set of basis functions used to project the residual onto the space of test functions.

The selection of basis functions for both spaces is crucial for ensuring the accuracy and computational efficiency of the discretization. **Trial Spaces:**

$$U \approx U_h, \quad V \approx V_h, \quad W \approx W_h \quad \text{and} \quad P \approx P_h.$$

Test Spaces:

$$\bar{W} \approx \bar{W}_h \quad \text{and} \quad Q \approx Q_h.$$

Find

$$(U_h, V_h, W_h) \in \bar{W}_h \quad \text{and} \quad P_h \in Q_h$$

such that

$$\begin{aligned} & \frac{1}{\delta t} \int_{\Omega^{n+1}} U_h^{n+1} \tilde{U}_h d\Omega - \frac{1}{\delta t} \left(U_h^n \circ X^n \right) \tilde{U}_h d\Omega + q_h \int_{\Omega^{n+1}} U_h^{n+1} \frac{\partial \tilde{U}_h}{\partial X^{n+1}} d\Omega - P_h^{n+1} \int_{\Omega^{n+1}} \frac{\partial \tilde{U}_h}{\partial X^{n+1}} d\Omega - \\ & \frac{1}{Re} (1 + K) \left\{ - \int_{\Omega^{n+1}} \frac{\partial U_h^{n+1}}{\partial X^{n+1}} \frac{\partial \tilde{U}_h}{\partial X^{n+1}} d\Omega \right. \\ & \left. + \oint_{\Gamma} \tilde{U}_h \left(n_x \frac{\partial U_h^{n+1}}{\partial X^{n+1}} \right) d\Gamma - \int_{\Omega^{n+1}} \frac{\partial U_h^{n+1}}{\partial Y^{n+1}} \frac{\partial \tilde{U}_h}{\partial Y^{n+1}} d\Omega + \oint_{\Gamma} \tilde{U}_h \left(n_y \frac{\partial U_h^{n+1}}{\partial Y^{n+1}} \right) d\Gamma \right\} \\ & + \frac{K}{Re} \int_{\Omega^{n+1}} W_h^{n+1} \frac{\partial \tilde{U}_h}{\partial Y^{n+1}} d\Omega + \frac{\alpha}{2} \int_{\Omega^{n+1}} (V_h^{n+1} W_h^n + V_h^n W_h^{n+1}) \tilde{U}_h d\Omega + \\ & \frac{\beta}{2} \int_{\Omega^{n+1}} (U_h^{n+1} W_h^{2n} + U_h^n W_h^{2n+2}) \tilde{U}_h d\Omega = 0 \end{aligned} \tag{4.20}$$

$$\begin{aligned}
& \frac{1}{\delta t} \int_{\Omega^{n+1}} V_h^{n+1} \tilde{V}_h d\Omega - \frac{1}{\delta t} \left(V_h^n \circ Y^n \right) \tilde{V}_h d\Omega + q_h \int_{\Omega^{n+1}} V_h^{n+1} \frac{\partial \tilde{V}_h}{\partial Y^{n+1}} d\Omega \\
& - P_h^{n+1} \int_{\Omega^{n+1}} \frac{\partial \tilde{V}_h}{\partial Y^{n+1}} d\Omega - \\
& \frac{1}{Re} (1 + K) \left\{ - \int_{\Omega^{n+1}} \frac{\partial V_h^{n+1}}{\partial X^{n+1}} \frac{\partial \tilde{V}_h}{\partial X^{n+1}} d\Omega \right. \\
& + \oint_{\Gamma} \tilde{V}_h \left(n_x \frac{\partial V_h^{n+1}}{\partial X^{n+1}} \right) d\Gamma - \\
& \left. \int_{\Omega^{n+1}} \frac{\partial V_h^{n+1}}{\partial Y^{n+1}} \frac{\partial \tilde{V}_h}{\partial Y^{n+1}} d\Omega + \oint_{\Gamma} \tilde{V}_h \left(n_y \frac{\partial V_h^{n+1}}{\partial Y^{n+1}} \right) d\Gamma \right\} \\
& - \frac{K}{Re} \int_{\Omega^{n+1}} W_h^{n+1} \frac{\partial \tilde{V}_h}{\partial X^{n+1}} d\Omega + \frac{\alpha}{2} \int_{\Omega^{n+1}} (U_h^{n+1} W_h^n + U_h^n W_h^{n+1}) \tilde{V}_h d\Omega + \\
& \left(\frac{\alpha^2}{\beta} \right) \int_{\Omega^{n+1}} V_h^{n+1} \tilde{V}_h d\Omega = 0
\end{aligned} \tag{4.21}$$

$$\begin{aligned}
& \frac{1}{\delta t} \int_{\Omega^{n+1}} W_h^{n+1} \tilde{W}_h d\Omega - \frac{1}{\delta t} \left(W_h^n \circ X^n \right) \tilde{W}_h d\Omega \\
& - \frac{1}{Re} \left(1 + \frac{K}{2} \right) \left\{ - \int_{\Omega^{n+1}} \frac{\partial W_h^{n+1}}{\partial X^{n+1}} \frac{\partial \tilde{W}_h}{\partial X^{n+1}} d\Omega + \oint_{\Gamma} \tilde{W}_h \left(n_x \frac{\partial W_h^{n+1}}{\partial X^{n+1}} \right) d\Gamma \right. \\
& - \left. \int_{\Omega^{n+1}} \frac{\partial W_h^{n+1}}{\partial Y^{n+1}} \frac{\partial \tilde{W}_h}{\partial Y^{n+1}} d\Omega + \oint_{\Gamma} \tilde{W}_h \left(n_y \frac{\partial W_h^{n+1}}{\partial Y^{n+1}} \right) d\Gamma \right\} \\
& - \frac{2K}{Re E_r} \int_{\Omega^{n+1}} \left(- V_h^{n+1} \frac{\partial \tilde{W}_h}{\partial X^{n+1}} + U_h^{n+1} \frac{\partial \tilde{W}_h}{\partial Y^{n+1}} - 2 W_h^{n+1} \tilde{W}_h \right) d\Omega = 0
\end{aligned} \tag{4.22}$$

for all $\tilde{U}_h, \tilde{V}_h, \tilde{W}_h \in \bar{W}_h$ and $P_h \in Q_h$.

FEM approximation is achieved by using the approximate trial solution functions and trial test functions. These functions are the linear combination of nodal unknowns and shape functions which are linearly independent. Given below are the trial solution functions:

$$U_h = \sum_{j=1}^m U_j \xi_j, \quad V_h = \sum_{j=1}^m V_j \xi_j, \quad W_h = \sum_{j=1}^m W_j \xi_j, \quad P_h = \sum_{j=1}^l P_j \eta_j.$$

In all above relations ξ_j and η_j are the shape functions. By using these approximations in Eqs. (4.20) to (4.22), weak formulation can be expressed as

(4.20) \Rightarrow

$$\begin{aligned}
& \frac{1}{\delta t} \int_{\Omega^{n+1}} \left(\sum_{j=1}^m U_j \xi_j \right)^{n+1} \sum_{i=1}^m \tilde{U}_i \xi_i d\Omega - \frac{1}{\delta t} \left(\left(\sum_{j=1}^m U_j \xi_j \right)^n \circ X^n \right) \sum_{i=1}^m \tilde{U}_i \xi_i d\Omega \\
& + \sum_{i=1}^l q_i \xi_i \int_{\Omega^{n+1}} \sum_{j=1}^m U_j \xi_j \frac{\partial}{\partial X} \sum_{i=1}^m \tilde{U}_i \xi_i d\Omega - \sum_{j=1}^l P_j \eta_j \int_{\Omega^{n+1}} \frac{\partial}{\partial X} \sum_{i=1}^m \tilde{U}_i \xi_i d\Omega \\
& - \frac{1}{Re} (1+K) \left\{ - \int_{\Omega^{n+1}} \frac{\partial}{\partial X} \sum_{j=1}^m U_j \xi_j \frac{\partial}{\partial X} \sum_{i=1}^m \tilde{U}_i \xi_i d\Omega + \oint_{\Gamma} \sum_{i=1}^m \tilde{U}_i \xi_i \left(n_x \frac{\partial}{\partial X} \sum_{j=1}^m U_j \xi_j \right) d\Gamma \right. \\
& \left. - \int_{\Omega^{n+1}} \frac{\partial}{\partial Y} \sum_{j=1}^m U_j \xi_j \frac{\partial}{\partial Y} \sum_{i=1}^m \tilde{U}_i \xi_i d\Omega + \oint_{\Gamma} \sum_{i=1}^m \tilde{U}_i \xi_i \left(n_y \frac{\partial}{\partial Y} \sum_{j=1}^m U_j \xi_j \right) d\Gamma \right\} \\
& + \frac{K}{Re} \int_{\Omega^{n+1}} \sum_{j=1}^m W_j \xi_j \frac{\partial}{\partial Y} \sum_{i=1}^m \tilde{U}_i \xi_i d\Omega + \frac{\alpha}{2} \int_{\Omega^{n+1}} \left(\left(\sum_{j=1}^m V_j \xi_j \right)^{n+1} \left(\sum_{j=1}^m W_j \xi_j \right)^n \right. \\
& \left. + \left(\sum_{j=1}^m V_j \xi_j \right)^n \left(\sum_{j=1}^m W_j \xi_j \right)^{n+1} \right) \sum_{i=1}^m \tilde{U}_i \xi_i d\Omega + \frac{\beta}{2} \int_{\Omega^{n+1}} \left(\left(\sum_{j=1}^m U_j \xi_j \right)^{n+1} \left(\sum_{j=1}^m W_j \xi_j \right)^{2n} \right. \\
& \left. + \left(\sum_{j=1}^m U_j \xi_j \right)^n \left(\sum_{j=1}^m W_j \xi_j \right)^{2n+2} \right) \sum_{i=1}^m \tilde{U}_i \xi_i d\Omega = 0
\end{aligned}$$

By Galerkins,

$$\tilde{U}_h = \sum_{i=1}^m \xi_i$$

$$\begin{aligned}
& \frac{1}{\delta t} \int_{\Omega^{n+1}} \left(\sum_{j=1}^m U_j \xi_j \right)^{n+1} \sum_{i=1}^m \xi_i d\Omega - \frac{1}{\delta t} \left(\left(\sum_{j=1}^m U_j \xi_j \right)^n \circ X^n \right) \sum_{i=1}^m \xi_i d\Omega \\
& + \sum_{i=1}^l q_i \xi_i \int_{\Omega^{n+1}} \sum_{j=1}^m U_j \xi_j \frac{\partial}{\partial X} \sum_{i=1}^m \xi_i d\Omega - \sum_{j=1}^l P_j \eta_j \int_{\Omega^{n+1}} \frac{\partial}{\partial X} \sum_{i=1}^m \xi_i d\Omega \\
& - \frac{1}{Re} (1+K) \left\{ - \int_{\Omega^{n+1}} \frac{\partial}{\partial X} \sum_{j=1}^m U_j \xi_j \frac{\partial}{\partial X} \sum_{i=1}^m \xi_i d\Omega + \oint_{\Gamma} \sum_{i=1}^m \xi_i \left(n_x \frac{\partial}{\partial X} \sum_{j=1}^m U_j \xi_j \right) d\Gamma \right. \\
& \left. - \int_{\Omega^{n+1}} \frac{\partial}{\partial Y} \sum_{j=1}^m U_j \xi_j \frac{\partial}{\partial Y} \sum_{i=1}^m \xi_i d\Omega + \oint_{\Gamma} \sum_{i=1}^m \xi_i \left(n_y \frac{\partial}{\partial Y} \sum_{j=1}^m U_j \xi_j \right) d\Gamma \right\} \\
& + \frac{K}{Re} \int_{\Omega^{n+1}} \sum_{j=1}^m W_j \xi_j \frac{\partial}{\partial Y} \sum_{i=1}^m \xi_i d\Omega + \frac{\alpha}{2} \int_{\Omega^{n+1}} \left(\left(\sum_{j=1}^m V_j \xi_j \right)^{n+1} \left(\sum_{j=1}^m W_j \xi_j \right)^n \right. \\
& \left. + \left(\sum_{j=1}^m V_j \xi_j \right)^n \left(\sum_{j=1}^m W_j \xi_j \right)^{n+1} \right) \sum_{i=1}^m \xi_i d\Omega + \frac{\beta}{2} \int_{\Omega^{n+1}} \left(\left(\sum_{j=1}^m U_j \xi_j \right)^{n+1} \right. \\
& \left. \left(\sum_{j=1}^m W_j \xi_j \right)^{2n} + \left(\sum_{j=1}^m U_j \xi_j \right)^n \left(\sum_{j=1}^m W_j \xi_j \right)^{2n+2} \right) \sum_{i=1}^m \xi_i d\Omega = 0
\end{aligned}$$

$$\begin{aligned}
& \frac{1}{\delta t} \int_{\Omega^{n+1}} \left(\sum_{j=1}^m U_j \xi_j \right)^{n+1} \sum_{i=1}^m \xi_i d\Omega - \frac{1}{\delta t} \left(\left(\sum_{j=1}^m U_j \xi_j \right)^n \circ X^n \right) \sum_{i=1}^m \xi_i d\Omega \\
& + \sum_{i=1}^l q_i \xi_i \int_{\Omega^{n+1}} \sum_{j=1}^m U_j \xi_j \sum_{i=1}^m \frac{\partial \xi_i}{\partial X} d\Omega - \sum_{j=1}^l P_j \eta_j \int_{\Omega^{n+1}} \sum_{i=1}^m \frac{\partial \xi_i}{\partial X} d\Omega - \\
& \frac{1}{Re} (1+K) \left\{ - \int_{\Omega^{n+1}} \sum_{j=1}^m \frac{\partial \xi_j}{\partial X} U_j \sum_{i=1}^m \frac{\partial \xi_i}{\partial X} d\Omega + \oint_{\Gamma} \sum_{i=1}^m \xi_i \left(n_x \sum_{j=1}^m \frac{\partial \xi_j}{\partial X} U_j \right) d\Gamma \right. \\
& \left. - \int_{\Omega^{n+1}} \sum_{j=1}^m \frac{\partial \xi_j}{\partial Y} U_j \sum_{i=1}^m \frac{\partial \xi_i}{\partial Y} d\Omega + \oint_{\Gamma} \sum_{i=1}^m \xi_i \left(n_y \sum_{j=1}^m \frac{\partial \xi_j}{\partial Y} U_j \right) d\Gamma \right\} \\
& + \frac{K}{Re} \int_{\Omega^{n+1}} \sum_{j=1}^m W_j \xi_j \sum_{i=1}^m \frac{\partial \xi_i}{\partial Y} d\Omega + \frac{\alpha}{2} \int_{\Omega^{n+1}} \left(\left(\sum_{j=1}^m V_j \xi_j \right)^{n+1} \left(\sum_{j=1}^m W_j \xi_j \right)^n \right. \\
& \left. + \left(\sum_{j=1}^m V_j \xi_j \right)^n \left(\sum_{j=1}^m W_j \xi_j \right)^{n+1} \right) \sum_{i=1}^m \xi_i d\Omega + \frac{\beta}{2} \int_{\Omega^{n+1}} \left(\left(\sum_{j=1}^m U_j \xi_j \right)^{n+1} \left(\sum_{j=1}^m W_j \xi_j \right)^{2n} \right. \\
& \left. + \left(\sum_{j=1}^m U_j \xi_j \right)^n \left(\sum_{j=1}^m W_j \xi_j \right)^{2n+2} \right) \sum_{i=1}^m \xi_i d\Omega = 0
\end{aligned}$$

$$\begin{aligned}
& \frac{1}{\delta t} \int_{\Omega^{n+1}} \left(U_j \xi_j \right)^{n+1} \xi_i d\Omega - \\
& \frac{1}{\delta t} \left(\left(U_j \xi_j \right)^n \circ X^n \right) \xi_i d\Omega + \xi_i \\
& \int_{\Omega^{n+1}} \xi_j \frac{\partial \xi_i}{\partial X} d\Omega \\
& - \eta_j \int_{\Omega^{n+1}} \frac{\partial \xi_i}{\partial X} d\Omega - \frac{1}{Re} (1+K) \left\{ - \int_{\Omega^{n+1}} \frac{\partial \xi_j}{\partial X} \frac{\partial \xi_i}{\partial X} d\Omega - \right. \\
& \left. \int_{\Omega^{n+1}} \frac{\partial \xi_j}{\partial Y} \frac{\partial \xi_i}{\partial Y} d\Omega \right\} \\
& + \frac{K}{Re} \int_{\Omega^{n+1}} W_j \xi_j \\
& \frac{\partial \xi_i}{\partial Y} d\Omega + \frac{\alpha}{2} \int_{\Omega^{n+1}} \\
& \left(\left(V_j \xi_j \right)^{n+1} \left(W_j \xi_j \right)^n + \left(V_j \xi_j \right)^n \left(W_j \xi_j \right)^{n+1} \right) \xi_i d\Omega \\
& + \frac{\beta}{2} \int_{\Omega^{n+1}} \left(\left(U_j \xi_j \right)^{n+1} \left(W_j \xi_j \right)^{2n} + \left(U_j \xi_j \right)^n \left(W_j \xi_j \right)^{2n+2} \right) \xi_i d\Omega \\
& = \oint_{\Gamma} \xi_i \left(n_x \frac{\partial \xi_j}{\partial X} \right) d\Gamma + \oint_{\Gamma} \xi_i \left(n_y \frac{\partial \xi_j}{\partial Y} \right) d\Gamma
\end{aligned}$$

$$\begin{aligned}
& \frac{1}{\delta t} \int_{\Omega^{n+1}} U_j^{n+1} \xi_j^{n+1} \xi_i^{n+1} d\Omega - \frac{1}{\delta t} \left(U_j^n \xi_j^n \circ X^n \right) \xi_i^{n+1} d\Omega + \xi_i^{n+1} \int_{\Omega^{n+1}} \xi_j^{n+1} \frac{\partial \xi_i^{n+1}}{\partial X^{n+1}} d\Omega \\
& - \eta_j^{n+1} \int_{\Omega^{n+1}} \frac{\partial \xi_i^{n+1}}{\partial X^{n+1}} d\Omega - \frac{1}{Re} (1+K) \left\{ - \int_{\Omega^{n+1}} \frac{\partial \xi_j^{n+1}}{\partial X^{n+1}} \frac{\partial \xi_i^{n+1}}{\partial X^{n+1}} d\Omega \right. \\
& \left. - \int_{\Omega^{n+1}} \frac{\partial \xi_j^{n+1}}{\partial Y^{n+1}} \frac{\partial \xi_i^{n+1}}{\partial Y^{n+1}} d\Omega \right\} + \frac{K}{Re} \int_{\Omega^{n+1}} W_j^{n+1} \xi_j^{n+1} \frac{\partial \xi_i^{n+1}}{\partial Y^{n+1}} d\Omega \\
& + \frac{\alpha}{2} \int_{\Omega^{n+1}} \left(V_j^{n+1} \xi_j^{n+1} W_j^n \xi_j^n + V_j^n \xi_j^n W_j^{n+1} \xi_j^{n+1} \right) \xi_i^{n+1} d\Omega \\
& + \frac{\beta}{2} \int_{\Omega^{n+1}} \left(U_j^{n+1} \xi_j^{n+1} W_j^{2n} \xi_j^{2n} + U_j^n \xi_j^n W_j^{2n+2} \xi_j^{2n+2} \right) \xi_i^{n+1} d\Omega \\
& = \oint_{\Gamma} \xi_i^{n+1} \left(n_x \frac{\partial \xi_j^{n+1}}{\partial X^{n+1}} \right) d\Gamma + \oint_{\Gamma} \xi_i^{n+1} \left(n_y \frac{\partial \xi_j^{n+1}}{\partial Y^{n+1}} \right) d\Gamma
\end{aligned} \tag{4.23}$$

$$\begin{aligned}
& \frac{1}{\delta t} \int_{\Omega^{n+1}} \left(\sum_{j=1}^m V_j \xi_j \right)^{n+1} \sum_{i=1}^m \tilde{V}_i \xi_i d\Omega - \frac{1}{\delta t} \left(\left(\sum_{j=1}^m V_j \xi_j \right)^n \circ Y^n \right) \sum_{i=1}^m \tilde{V}_i \xi_i d\Omega \\
& + \sum_{i=1}^l q_i \xi_i \int_{\Omega^{n+1}} \sum_{j=1}^m V_j \xi_j \frac{\partial}{\partial Y} \sum_{i=1}^m \tilde{V}_i \xi_i d\Omega - \sum_{j=1}^l P_j \eta_j \int_{\Omega^{n+1}} \frac{\partial}{\partial Y} \sum_{i=1}^m \tilde{V}_i \xi_i d\Omega \\
& - \frac{1}{Re} (1+K) \left\{ - \int_{\Omega^{n+1}} \frac{\partial}{\partial X} \sum_{j=1}^m V_j \xi_j \frac{\partial}{\partial X} \sum_{i=1}^m \tilde{V}_i \xi_i d\Omega + \oint_{\Gamma} \sum_{i=1}^m \tilde{V}_i \xi_i \left(n_x \frac{\partial}{\partial X} \sum_{j=1}^m V_j \xi_j \right) d\Gamma \right. \\
& \left. - \int_{\Omega^{n+1}} \frac{\partial}{\partial Y} \sum_{j=1}^m V_j \xi_j \frac{\partial}{\partial Y} \sum_{i=1}^m \tilde{V}_i \xi_i d\Omega + \oint_{\Gamma} \sum_{i=1}^m \tilde{V}_i \xi_i \left(n_y \frac{\partial}{\partial Y} \sum_{j=1}^m V_j \xi_j \right) d\Gamma \right\} \\
& - \frac{K}{Re} \int_{\Omega^{n+1}} \sum_{j=1}^m W_j \xi_j \frac{\partial}{\partial X} \sum_{i=1}^m \tilde{V}_i \xi_i d\Omega + \frac{\alpha}{2} \int_{\Omega^{n+1}} \left(\left(\sum_{j=1}^m U_j \xi_j \right)^{n+1} \left(\sum_{j=1}^m W_j \xi_j \right)^n \right. \\
& \left. + \left(\sum_{j=1}^m U_j \xi_j \right)^{n+1} \left(\sum_{j=1}^m U_j \xi_j \right)^{n+1} \right) \sum_{i=1}^m \tilde{V}_i \xi_i d\Omega + \\
& \left(\frac{\alpha^2}{\beta} \right) \int_{\Omega^{n+1}} \sum_{j=1}^m V_j \xi_j \sum_{i=1}^m \tilde{V}_i \xi_i d\Omega = 0
\end{aligned}$$

By Galerkins,

$$\tilde{V}_h = \sum_{i=1}^m \xi_i$$

$$\begin{aligned}
& \frac{1}{\delta t} \int_{\Omega^{n+1}} \left(\sum_{j=1}^m V_j \xi_j \right)^{n+1} \sum_{i=1}^m \xi_i d\Omega - \frac{1}{\delta t} \left(\left(\sum_{j=1}^m V_j \xi_j \right)^n \cdot Y^n \right) \sum_{i=1}^m \xi_i d\Omega \\
& + \sum_{i=1}^l q_i \xi_i \int_{\Omega^{n+1}} \left(\sum_{j=1}^m V_j \xi_j \right) \left(\sum_{i=1}^m \frac{\partial \xi_i}{\partial Y} \right) d\Omega - \sum_{j=1}^l P_j \eta_j \int_{\Omega^{n+1}} \sum_{i=1}^m \frac{\partial \xi_i}{\partial Y} d\Omega \\
& - \frac{1}{Re} (1 + K) \left\{ - \int_{\Omega^{n+1}} \left(\sum_{j=1}^m \frac{\partial \xi_j}{\partial X} V_j \right) \left(\sum_{i=1}^m \frac{\partial \xi_i}{\partial X} \right) d\Omega + \oint_{\Gamma} \sum_{i=1}^m \xi_i \left(n_x \sum_{j=1}^m \frac{\partial \xi_j}{\partial X} V_j \right) d\Gamma \right. \\
& \left. - \int_{\Omega^{n+1}} \left(\sum_{j=1}^m \frac{\partial \xi_j}{\partial Y} V_j \right) \left(\sum_{i=1}^m \frac{\partial \xi_i}{\partial Y} \right) d\Omega + \oint_{\Gamma} \sum_{i=1}^m \xi_i \left(n_y \sum_{j=1}^m \frac{\partial \xi_j}{\partial Y} V_j \right) d\Gamma \right\} \\
& - \frac{K}{Re} \int_{\Omega^{n+1}} \left(\sum_{j=1}^m W_j \xi_j \right) \left(\sum_{i=1}^m \frac{\partial \xi_i}{\partial X} \right) d\Omega \\
& + \frac{\alpha}{2} \int_{\Omega^{n+1}} \left[\left(\sum_{j=1}^m U_j \xi_j \right)^{n+1} \left(\sum_{j=1}^m W_j \xi_j \right)^n \right. \\
& \left. + \left(\sum_{j=1}^m U_j \xi_j \right)^n \left(\sum_{j=1}^m U_j \xi_j \right)^{n+1} \sum_{i=1}^m \xi_i d\Omega + \left(\frac{\alpha^2}{\beta} \right) \int_{\Omega^{n+1}} \left(\sum_{j=1}^m V_j \xi_j \right) \left(\sum_{i=1}^m \xi_i \right) d\Omega = 0
\end{aligned}$$

$$\begin{aligned}
& \frac{1}{\delta t} \int_{\Omega^{n+1}} \left(V_j \xi_j \right)^{n+1} \xi_i d\Omega - \frac{1}{\delta t} \left(\left(V_j \xi_j \right)^n \circ Y^n \right) \xi_i d\Omega \\
& + \xi_i \int_{\Omega^{n+1}} \xi_j \frac{\partial \xi_i}{\partial Y} d\Omega \\
& - \eta_j \int_{\Omega^{n+1}} \frac{\partial \xi_i}{\partial Y} d\Omega - \frac{1}{Re} (1 + K) \\
& \left\{ - \int_{\Omega^{n+1}} \frac{\partial \xi_j}{\partial X} \frac{\partial \xi_i}{\partial X} d\Omega - \int_{\Omega^{n+1}} \frac{\partial \xi_j}{\partial Y} \frac{\partial \xi_i}{\partial Y} d\Omega \right\} \\
& - \frac{K}{Re} \int_{\Omega^{n+1}} W_j \xi_j \frac{\partial \xi_i}{\partial X} d\Omega + \\
& \frac{\alpha}{2} \int_{\Omega^{n+1}} \left(\left(U_j \xi_j \right)^{n+1} \left(W_j \xi_j \right)^n \right. \\
& \left. + \left(U_j \xi_j \right)^n \left(U_j \xi_j \right)^{n+1} \right) \xi_i d\Omega + \left(\frac{\alpha^2}{\beta} \right) \int_{\Omega^{n+1}} V_j \xi_j \xi_i d\Omega \\
& = \oint_{\Gamma} \xi_i \left(n_x \frac{\partial \xi_j}{\partial X} \right) d\Gamma + \oint_{\Gamma} \xi_i \left(n_y \frac{\partial \xi_j}{\partial Y} \right) d\Gamma
\end{aligned}$$

$$\begin{aligned}
& \frac{1}{\delta t} \int_{\Omega^{n+1}} V_j^{n+1} \xi_j^{n+1} \xi_i^{n+1} d\Omega - \frac{1}{\delta t} \left(V_j^n \xi_j^n \circ Y^n \right) \xi_i^{n+1} d\Omega + \xi_i^{n+1} \int_{\Omega^{n+1}} \xi_j^{n+1} \frac{\partial \xi_i^{n+1}}{\partial Y^{n+1}} d\Omega \\
& - \eta_j^{n+1} \int_{\Omega^{n+1}} \frac{\partial \xi_i^{n+1}}{\partial Y^{n+1}} d\Omega - \frac{1}{Re} (1 + K) \\
& \left\{ - \int_{\Omega^{n+1}} \frac{\partial \xi_j^{n+1}}{\partial X^{n+1}} \frac{\partial \xi_i^{n+1}}{\partial X^{n+1}} d\Omega \right. \\
& \left. - \int_{\Omega^{n+1}} \frac{\partial \xi_j^{n+1}}{\partial Y^{n+1}} \frac{\partial \xi_i^{n+1}}{\partial Y^{n+1}} d\Omega \right\} \\
& - \frac{K}{Re} \int_{\Omega^{n+1}} W_j^{n+1} \xi_j^{n+1} \frac{\partial \xi_i^{n+1}}{\partial X^{n+1}} d\Omega \\
& + \frac{\alpha}{2} \int_{\Omega^{n+1}} \left(\left(U_j \xi_j \right)^{n+1} \left(W_j \xi_j \right)^n + \left(U_j \xi_j \right)^n \left(U_j \xi_j \right)^{n+1} \right) \xi_i d\Omega \\
& + \left(\frac{\alpha^2}{\beta} \right) \int_{\Omega^{n+1}} V_j \xi_j \xi_i d\Omega = \oint_{\Gamma} \xi_i^{n+1} \left(n_x \frac{\partial \xi_j^{n+1}}{\partial X^{n+1}} \right) d\Gamma \\
& + \oint_{\Gamma} \xi_i^{n+1} \left(n_y \frac{\partial \xi_j^{n+1}}{\partial Y^{n+1}} \right) d\Gamma
\end{aligned} \tag{4.24}$$

(4.22) \Rightarrow

$$\begin{aligned}
& \frac{1}{\delta t} \int_{\Omega^{n+1}} \left(\sum_{j=1}^m W_j \xi_j \right)^{n+1} \sum_{i=1}^m \tilde{W}_i \xi_i d\Omega - \frac{1}{\delta t} \left(\left(\sum_{j=1}^m W_j \xi_j \right)^n \circ X^n \right) \sum_{i=1}^m \tilde{W}_i \xi_i d\Omega \\
& - \frac{1}{Re} \left(1 + \frac{K}{2} \right) \left\{ - \int_{\Omega^{n+1}} \frac{\partial}{\partial X} \sum_{j=1}^m W_j \xi_j \frac{\partial}{\partial X} \sum_{i=1}^m \tilde{W}_i \xi_i d\Omega \right. \\
& + \oint_{\Gamma} \sum_{i=1}^m \tilde{W}_i \xi_i \left(n_x \frac{\partial}{\partial X} \sum_{j=1}^m W_j \xi_j \right) d\Gamma - \int_{\Omega^{n+1}} \frac{\partial}{\partial Y} \sum_{j=1}^m W_j \xi_j \frac{\partial}{\partial Y} \sum_{i=1}^m \tilde{W}_i \xi_i d\Omega \\
& \left. + \oint_{\Gamma} \sum_{i=1}^m \tilde{W}_i \xi_i \left(n_y \frac{\partial}{\partial Y} \sum_{j=1}^m W_j \xi_j \right) d\Gamma \right\} - \frac{2K}{Re E_r} \int_{\Omega^{n+1}} \left(- \sum_{j=1}^m V_j \xi_j \frac{\partial}{\partial X} \sum_{i=1}^m \tilde{W}_i \xi_i \right. \\
& \left. + \sum_{j=1}^m U_j \xi_j \frac{\partial}{\partial Y} \sum_{i=1}^m \tilde{W}_i \xi_i - 2 \sum_{j=1}^m W_j \xi_j \sum_{i=1}^m \tilde{W}_i \xi_i \right) d\Omega = 0
\end{aligned}$$

By Galerkins,

$$\tilde{W}_h = \sum_{i=1}^m \xi_i$$

$$\begin{aligned}
& \frac{1}{\delta t} \int_{\Omega^{n+1}} \left(\sum_{j=1}^m W_j \xi_j \right)^{n+1} \sum_{i=1}^m \xi_i d\Omega - \frac{1}{\delta t} \left(\left(\sum_{j=1}^m W_j \xi_j \right)^n \circ X^n \right) \sum_{i=1}^m \xi_i d\Omega \\
& - \frac{1}{Re} \left(1 + \frac{K}{2} \right) \left\{ \int_{\Omega^{n+1}} \frac{\partial}{\partial X} \sum_{j=1}^m W_j \xi_j \frac{\partial}{\partial X} \sum_{i=1}^m \xi_i d\Omega \right. \\
& + \oint_{\Gamma} \sum_{i=1}^m \xi_i \left(n_x \frac{\partial}{\partial X} \sum_{j=1}^m W_j \xi_j \right) d\Gamma - \int_{\Omega^{n+1}} \frac{\partial}{\partial Y} \sum_{j=1}^m W_j \xi_j \frac{\partial}{\partial Y} \sum_{i=1}^m \xi_i d\Omega \\
& \left. + \oint_{\Gamma} \sum_{i=1}^m \xi_i \left(n_y \frac{\partial}{\partial Y} \sum_{j=1}^m W_j \xi_j \right) d\Gamma \right\} - \frac{2K}{Re E_r} \int_{\Omega^{n+1}} \left(- \sum_{j=1}^m V_j \xi_j \frac{\partial}{\partial X} \sum_{i=1}^m \xi_i \right. \\
& \left. + \sum_{j=1}^m U_j \xi_j \frac{\partial}{\partial Y} \sum_{i=1}^m \xi_i - 2 \sum_{j=1}^m W_j \xi_j \sum_{i=1}^m \xi_i \right) d\Omega = 0
\end{aligned}$$

$$\begin{aligned}
& \frac{1}{\delta t} \int_{\Omega^{n+1}} \left(\sum_{j=1}^m W_j \xi_j \right)^{n+1} \sum_{i=1}^m \xi_i d\Omega - \frac{1}{\delta t} \left(\left(\sum_{j=1}^m W_j \xi_j \right)^n \circ X^n \right) \sum_{i=1}^m \xi_i d\Omega \\
& - \frac{1}{Re} \left(1 + \frac{K}{2} \right) \left\{ - \int_{\Omega^{n+1}} \sum_{j=1}^m \frac{\partial \xi_j}{\partial X} W_j \sum_{i=1}^m \frac{\partial \xi_i}{\partial X} d\Omega + \oint_{\Gamma} \sum_{i=1}^m \xi_i \left(n_x \sum_{j=1}^m \frac{\partial \xi_j}{\partial X} W_j \right) d\Gamma \right. \\
& \left. - \int_{\Omega^{n+1}} \sum_{j=1}^m \frac{\partial \xi_j}{\partial Y} W_j \sum_{i=1}^m \frac{\partial \xi_i}{\partial Y} d\Omega + \oint_{\Gamma} \sum_{i=1}^m \xi_i \left(n_y \sum_{j=1}^m \frac{\partial \xi_j}{\partial Y} W_j \right) d\Gamma \right\} \\
& - \frac{2K}{Re E_r} \int_{\Omega^{n+1}} \left(\sum_{j=1}^m V_j \xi_j \sum_{i=1}^m \frac{\partial \xi_i}{\partial X} + \sum_{j=1}^m U_j \xi_j \sum_{i=1}^m \frac{\partial \xi_i}{\partial Y} - 2 \sum_{j=1}^m W_j \xi_j \sum_{i=1}^m \xi_i \right) d\Omega = 0
\end{aligned}$$

$$\begin{aligned}
& \frac{1}{\delta t} \int_{\Omega^{n+1}} \left(W_j \xi_j \right)^{n+1} \xi_i d\Omega - \frac{1}{\delta t} \left(\left(W_j \xi_j \right)^n \circ X^n \right) \xi_i d\Omega \\
& - \frac{1}{Re} \left(1 + \frac{K}{2} \right) \left\{ - \int_{\Omega^{n+1}} \frac{\partial \xi_j}{\partial X} \frac{\partial \xi_i}{\partial X} d\Omega - \int_{\Omega^{n+1}} \frac{\partial \xi_j}{\partial Y} \frac{\partial \xi_i}{\partial Y} d\Omega \right\} \\
& - \frac{2K}{Re E_r} \int_{\Omega^{n+1}} \left(- \xi_j \frac{\partial \xi_i}{\partial X} + \xi_j \frac{\partial \xi_i}{\partial Y} - 2 \xi_j \xi_i \right) d\Omega = \oint_{\Gamma} \xi_i \left(n_x \frac{\partial \xi_j}{\partial X} \right) d\Gamma \\
& + \oint_{\Gamma} \xi_i \left(n_y \frac{\partial \xi_j}{\partial Y} \right) d\Gamma
\end{aligned}$$

$$\begin{aligned}
& \frac{1}{\delta t} \int_{\Omega^{n+1}} W_j^{n+1} \xi_j^{n+1} \xi_i^{n+1} d\Omega - \frac{1}{\delta t} \left(W_j^n \xi_j^n \circ X^n \right) \xi_i^{n+1} d\Omega \\
& - \frac{1}{Re} \left(1 + \frac{K}{2} \right) \left\{ - \int_{\Omega^{n+1}} \frac{\partial \xi_j^{n+1}}{\partial X^{n+1}} \frac{\partial \xi_i^{n+1}}{\partial X^{n+1}} d\Omega - \int_{\Omega^{n+1}} \frac{\partial \xi_j^{n+1}}{\partial Y^{n+1}} \frac{\partial \xi_i^{n+1}}{\partial Y^{n+1}} d\Omega \right\} \\
& - \frac{2K}{Re E_r} \int_{\Omega^{n+1}} \left(- \xi_j^{n+1} \frac{\partial \xi_i^{n+1}}{\partial X^{n+1}} + \xi_j^{n+1} \frac{\partial \xi_i^{n+1}}{\partial Y^{n+1}} - 2 \xi_j^{n+1} \xi_i^{n+1} \right) d\Omega \\
& = \oint_{\Gamma} \xi_i^{n+1} \left(n_x \frac{\partial \xi_j^{n+1}}{\partial X^{n+1}} \right) d\Gamma + \oint_{\Gamma} \xi_i^{n+1} \left(n_y \frac{\partial \xi_j^{n+1}}{\partial Y^{n+1}} \right) d\Gamma
\end{aligned} \tag{4.25}$$

From Eqs. (4.23) to (4.25), we get the discretized system of nonlinear algebraic equations as

$$[K^*(U, V)]\{X^*\} = \{Q^*\}.$$

The matrix notation of $K^*(U, V)$, X^* and Q^* can be written as

$$\underbrace{\begin{bmatrix} A_{11} & A_{12} & B_1 & A_{14} \\ A_{21} & A_{22} & B_2 & A_{24} \\ B_1^t & B_2^t & A_{33} & A_{34} \\ A_{41} & A_{42} & A_{43} & A_{44} \end{bmatrix}}_{K^*} \underbrace{\begin{bmatrix} U_h \\ V_h \\ P_h \\ W_h \end{bmatrix}}_{X^*} = \underbrace{\begin{bmatrix} Q_1 \\ Q_2 \\ Q_3 \\ Q_4 \end{bmatrix}}_{Q^*}. \tag{4.26}$$

Here K^* , X^* and Q^* are called block stiffness matrix, block solution vector and block boundary vector respectively.

The local elemental entries of block stiffness matrix are given as

$$\begin{aligned}
A_{11} &= \frac{1}{\delta t} \int_{\Omega^{n+1}} U_j^{n+1} \xi_j^{n+1} \xi_i^{n+1} d\Omega - \frac{1}{\delta t} \left(U_j^n \xi_j^n \circ X^n \right) \xi_i^{n+1} d\Omega \\
&+ \xi_i^{n+1} \int_{\Omega^{n+1}} \xi_j^{n+1} \frac{\partial \xi_i^{n+1}}{\partial X^{n+1}} d\Omega - \frac{1}{Re} (1 + K) \left\{ - \int_{\Omega^{n+1}} \frac{\partial \xi_j^{n+1}}{\partial X^{n+1}} \frac{\partial \xi_i^{n+1}}{\partial X^{n+1}} d\Omega \right. \\
&- \left. \int_{\Omega^{n+1}} \frac{\partial \xi_j^{n+1}}{\partial Y^{n+1}} \frac{\partial \xi_i^{n+1}}{\partial Y^{n+1}} d\Omega \right\} + \frac{\beta}{2} \int_{\Omega^{n+1}} \left(U_j^{n+1} \xi_j^{n+1} \right. \\
&\left. W_j^{2n} \xi_j^{2n} + U_j^n \xi_j^n W_j^{2n+2} \xi_j^{2n+2} \right) \xi_i^{n+1} d\Omega,
\end{aligned}$$

$$A_{12} = \frac{\alpha}{2} \int_{\Omega^{n+1}} \left(V_j^{n+1} \xi_j^{n+1} W_j^n \xi_j^n + V_j^n \xi_j^n W_j^{n+1} \xi_j^{n+1} \right) \xi_i^{n+1} d\Omega,$$

$$\begin{aligned} A_{14} &= \frac{K}{Re} \int_{\Omega^{n+1}} W_j^{n+1} \xi_j^{n+1} \frac{\partial \xi_i^{n+1}}{\partial Y^{n+1}} d\Omega \\ &+ \frac{\alpha}{2} \int_{\Omega^{n+1}} \left(V_j^{n+1} \xi_j^{n+1} W_j^n \xi_j^n + V_j^n \xi_j^n W_j^{n+1} \xi_j^{n+1} \right) \xi_i^{n+1} d\Omega + \\ &\frac{\beta}{2} \int_{\Omega^{n+1}} \left(U_j^{n+1} \xi_j^{n+1} W_j^{2n} \xi_j^{2n} + U_j^n \xi_j^n W_j^{2n+2} \xi_j^{2n+2} \right) \xi_i^{n+1} d\Omega, \end{aligned}$$

$$A_{21} = \frac{\alpha}{2} \int_{\Omega^{n+1}} \left(\left(U_j \xi_j \right)^{n+1} \left(W_j \xi_j \right)^n + \left(U_j \xi_j \right)^n \left(U_j \xi_j \right)^{n+1} \right) \xi_i d\Omega,$$

$$A_{22} = \frac{1}{\delta t} \int_{\Omega^{n+1}} V_j^{n+1} \xi_j^{n+1} \xi_i^{n+1} d\Omega - \frac{1}{\delta t} \left(V_j^n \xi_j^n \circ Y^n \right) \xi_i^{n+1} d\Omega + \xi_i^{n+1} \int_{\Omega^{n+1}} \xi_j^{n+1}$$

$$\begin{aligned} &\frac{\partial \xi_i^{n+1}}{\partial Y^{n+1}} d\Omega - \frac{1}{Re} (1 + K) \left\{ - \int_{\Omega^{n+1}} \frac{\partial \xi_j^{n+1}}{\partial X^{n+1}} \frac{\partial \xi_i^{n+1}}{\partial X^{n+1}} d\Omega \right. \\ &\left. - \int_{\Omega^{n+1}} \frac{\partial \xi_j^{n+1}}{\partial Y^{n+1}} \frac{\partial \xi_i^{n+1}}{\partial Y^{n+1}} d\Omega \right\} + \left(\frac{\alpha^2}{\beta} \right) \int_{\Omega^{n+1}} V_j \xi_j \xi_i d\Omega, \end{aligned}$$

$$\begin{aligned} A_{24} &= \frac{K}{Re} \int_{\Omega^{n+1}} W_j^{n+1} \xi_j^{n+1} \frac{\partial \xi_i^{n+1}}{\partial X^{n+1}} d\Omega + \frac{\alpha}{2} \int_{\Omega^{n+1}} \left(\left(U_j \xi_j \right)^{n+1} \left(W_j \xi_j \right)^n \right. \\ &\left. + \left(U_j \xi_j \right)^n \left(U_j \xi_j \right)^{n+1} \right) \xi_i d\Omega, \end{aligned}$$

$$A_{41} = \xi_j^{n+1} \frac{\partial \xi_i^{n+1}}{\partial Y^{n+1}},$$

$$\begin{aligned} A_{44} &= \frac{1}{\delta t} \int_{\Omega^{n+1}} W_j^{n+1} \xi_j^{n+1} \xi_i^{n+1} d\Omega - \frac{1}{\delta t} \left(W_j^n \xi_j^n \circ X^n \right) \xi_i^{n+1} d\Omega \\ &- \frac{1}{Re} \left(1 + \frac{K}{2} \right) \left\{ - \int_{\Omega^{n+1}} \frac{\partial \xi_j^{n+1}}{\partial X^{n+1}} \frac{\partial \xi_i^{n+1}}{\partial X^{n+1}} d\Omega - \int_{\Omega^{n+1}} \frac{\partial \xi_j^{n+1}}{\partial Y^{n+1}} \frac{\partial \xi_i^{n+1}}{\partial Y^{n+1}} d\Omega \right\} \\ &- \frac{2K}{Re E_r} \int_{\Omega^{n+1}} \left(- 2 \xi_j^{n+1} \xi_i^{n+1} \right) d\Omega \end{aligned}$$

$$A_{42} = -\xi_j^{n+1} \frac{\partial \xi_i^{n+1}}{\partial X^{n+1}},$$

$$A_{33} = 0,$$

$$A_{34} = 0,$$

$$A_{43} = 0.$$

The entries A_{13} , A_{23} and A_{31} , A_{32} are the pressure matrices with their respective transposes can be written as

$$B_1^{ij} = -\eta_j^{n+1} \int_{\Omega^{n+1}} \frac{\partial \xi_i^{n+1}}{\partial X^{n+1}} d\Omega,$$

$$B_2^{ij} = -\eta_j^{n+1} \int_{\Omega^{n+1}} \frac{\partial \xi_i^{n+1}}{\partial Y^{n+1}} d\Omega,$$

$$(B_1^{ij})^t = -\xi_i^{n+1} \int_{\Omega^{n+1}} \frac{\partial \eta_j^{n+1}}{\partial X^{n+1}} d\Omega,$$

$$(B_2^{ij})^t = -\xi_i^{n+1} \int_{\Omega^{n+1}} \frac{\partial \eta_j^{n+1}}{\partial Y^{n+1}} d\Omega,$$

$$Q_1 = \oint_{\Gamma} \xi_i^{n+1} \left(n_x \frac{\partial \xi_j^{n+1}}{\partial X^{n+1}} \right) d\Gamma + \oint_{\Gamma} \xi_i^{n+1} \left(n_y \frac{\partial \xi_j^{n+1}}{\partial Y^{n+1}} \right) d\Gamma,$$

$$Q_2 = \oint_{\Gamma} \xi_i^{n+1} \left(n_x \frac{\partial \xi_j^{n+1}}{\partial X^{n+1}} \right) d\Gamma + \oint_{\Gamma} \xi_i^{n+1} \left(n_y \frac{\partial \xi_j^{n+1}}{\partial Y^{n+1}} \right) d\Gamma,$$

$$Q_3 = 0,$$

$$Q_4 = \oint_{\Gamma} \xi_i^{n+1} \left(n_x \frac{\partial \xi_j^{n+1}}{\partial X^{n+1}} \right) d\Gamma + \oint_{\Gamma} \xi_i^{n+1} \left(n_y \frac{\partial \xi_j^{n+1}}{\partial Y^{n+1}} \right) d\Gamma.$$

The system of non-linear algebraic equations in discrete form can be expressed as follows:

$$\begin{bmatrix} A_{11} & A_{12} & B_1 & A_{14} \\ A_{21} & A_{22} & B_2 & A_{24} \\ B_1^T & B_2^T & 0 & 0 \\ A_{41} & A_{42} & 0 & A_{44} \end{bmatrix} \begin{bmatrix} U_h \\ V_h \\ P_h \\ W_h \end{bmatrix} = \begin{bmatrix} Q_1 \\ Q_2 \\ 0 \\ Q_4 \end{bmatrix} \quad (4.27)$$

An examination of the weak form Eqs. (4.20) to (4.22) and the finite element matrices in (4.26) shows that ξ_i should be at least linear functions of x and y . Selected two-dimensional finite elements are used to discretize the domain. This matrix is implemented in Free Fem++, the code is used to compute the solution for variant parameters on the computational domain.

4.6 Results and Discussion

In this chapter, numerical results are presented that are obtained through solving the presented model. The model is solved for the BFS problem geometry under consideration. The domain of the problem is discretized into 14640 number of elements. To compute the solution of the problem FEM is employed and the governing differential equations are solved over the computational mesh. In order to validate the computed solution Table 4.1 is presented where Reattachment lengths are computed. The reattachment lengths are computed for three different Reynolds number, i.e. for $Re = 50$, $Re = 150$ and $Re = 500$.

The computed solutions for the reattachment lengths are compared with the numerical solution obtained by Morgan et al. [32]. It is seen that the obtained numerical solution for the reattachment lengths is approximately close to the solution obtained in [32] for the three discussed Reynolds number. This clearly indicates that the presented model problem is coded efficiently and the results obtained by this code are accurate.

Re	Reattachment [32]	Reattachment Present
50	2.85	2.54
150	6.1	6.13
500	14.2	13.57

TABLE 4.1: Comparison of reattachment points with the literature.

Re	Reattachment without MMR	Reattachment with MMR
50	2.09327	1.74835
150	5.07213	4.79663
300	8.3155	8.15936
400	9.91214	9.63962
500	11.0214	10.7578

TABLE 4.2: Reattachment points with and without MMR effect.

In Figure 4.2, the stream lines of the velocity field are shown. The effect of micromagnetorotation (MMR) is computed for two different Reynold numbers. The Reynold numbers taken for this purpose are $Re = 50$ and $Re = 500$. In Figure 4.2(a) the stream lines are shown for $Re = 50$ without the consideration of

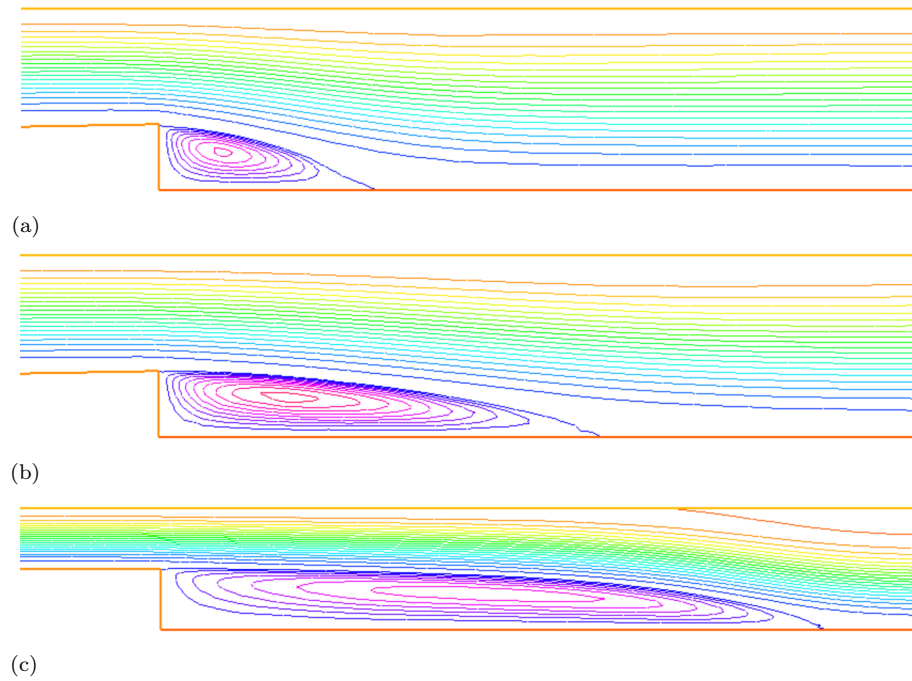


FIGURE 4.1: Velocity contours for varying Re with fine mesh. (a) For $Re = 50$
 (b) For $Re = 150$ (c) For $Re = 500$

Re	Ψ_{max} without MMR	Ψ_{max} with MMR
50	0.0137976	0.0113979
150	0.0199193	0.0197762
300	0.0214554	0.0214812
400	0.0218086	0.0219083
500	0.0219075	0.0219322

TABLE 4.3: Maximum Stream function values with and without MMR effect.

MMR effect, i.e. in this case the parameters α , β and aa are taken to be $\alpha = 0$, $\beta = 0$ and $aaa = 0$.

Whereas, Figure 4.2(b) is calculated with the consideration of the MMR effect, i.e. the parameters α , β and aa are taken to be $\alpha = 1$, $\beta = 1$ and $aaa = 1$. Figure 4.2(c) shows the stream lines for $Re = 500$ without the consideration of MMR effect. Whereas, Figure 4.2(d) is computed with the consideration of the MMR effect.

It is seen from these sub-figures that the reattachment point is higher in the case when there is no micromagnetorotation as compared to the case when the micromagnetorotation is considered. In the presence of MMR effect the flow is experiencing a resistance in flow speed due to magnetization effect which leads to the decrease in the reattachment length. Moreover, this decrement of the reattachment

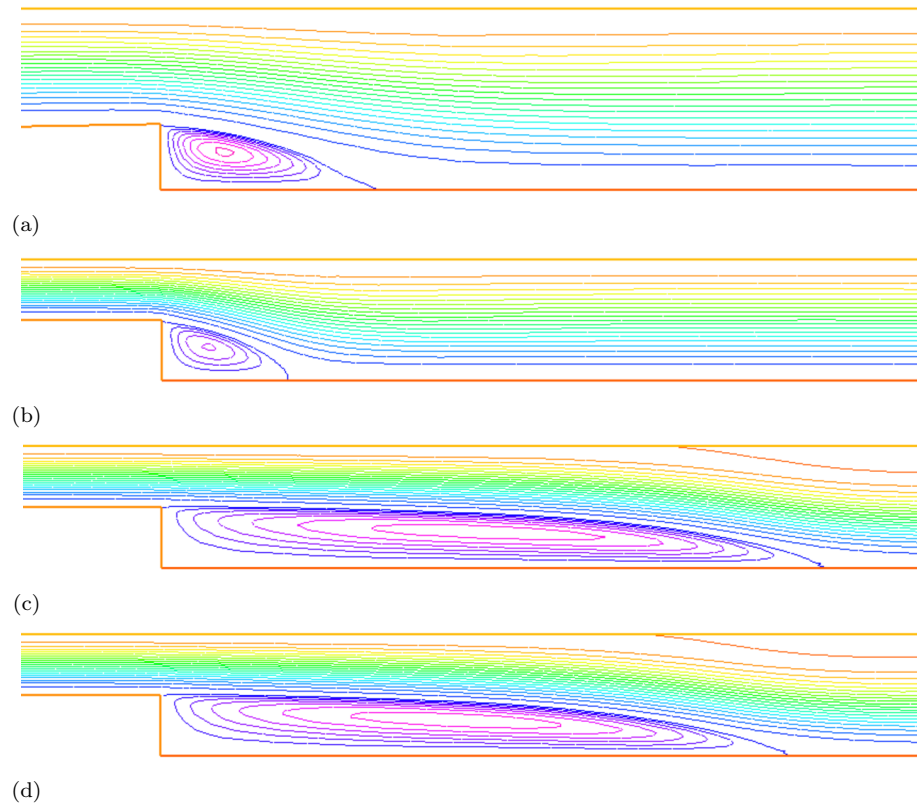


FIGURE 4.2: stream lines with and without MMR for different Reynolds number Re . (a) For $Re = 50$ without MMR (b) For $Re = 50$ with MMR (c) For $Re = 500$ without MMR (d) For $Re = 500$ with MMR

length with the consideration of magnetization MMR effect is more significant in the case of smaller Reynolds number as compared to the higher Reynolds number.

In Table 4.2, The reattachment points are computed for varying values of the Reynolds number. Both the cases where the MMR effect is taken into account and not are considered in these computations. The Reynolds numbers are varied from $Re = 50$ to $Re = 500$. It is observed that for increasing the Reynolds number the reattachment lengths increases in both the cases. The reattachment lengths in case when MMR is considered are always smaller than the reattachment lengths in the case when MMR is not taken into account. This is highly due to the resistance to the flow due to magnetization. Magnetization reduces the flow speed which leads to the difference in the formation of the primary vortex at the backward facing step in both the cases. In Table 4.3, the maximum values of the stream function are shown for varying values of the Reynolds number. The Reynolds numbers in this case are varied from $Re = 50$ to $Re = 500$. Both the cases where MMR is considered and the one without MMR is computed. It is observed

that the maximum value of the stream function is increasing with increasing the Reynolds number. Moreover, the maximum value of the stream function in case when the MMR is not present is higher than the maximum value of the stream function when the MMR effect is considered. Physically this is due to the effect of magnetization when the magnetization is considered the flow speed is reduced thus leads to lower stream function height.

Chapter 5

Conclusion and Future Work

In the present thesis, the classical backward-facing step (BFS) problem in fluid mechanics is re-examined within the framework of micropolar fluid dynamics, further augmented by the incorporation of micromagnetorotational (MMR) effects. To facilitate this investigation, a canonical two-dimensional BFS configuration is employed as a prototypical representation of the Navier–Stokes flow regime. Numerical approximations of the resultant velocity fields are subsequently derived through this construct. The foundational model is further generalized to encompass micropolar phenomena by coupling the governing micropolar equations with the conventional Navier–Stokes equations (NSE). Moreover, the mathematical framework is rigorously extended to integrate the influence of MMR dynamics, yielding a coupled system of nonlinear partial differential equations (PDEs) that encapsulate the enriched fluid behavior. To ensure physical fidelity, appropriate boundary conditions are meticulously prescribed for the BFS geometry. The complete dynamical system is therefore delineated through the ensemble of governing PDEs in conjunction with their associated boundary specifications. The numerical resolution of the formulated problem is executed via a finite element method (FEM) paradigm. Prior to discretization, the governing equations and boundary constraints undergo a systematic non-dimensionalization process to reduce the parametric complexity and to enhance computational tractability. Subsequently, the weak form of the non-dimensional PDE system is rigorously derived. The open-source computational platform FreeFEM++ is employed to implement the

deduced weak formulation. Validation of the computational implementation is conducted by benchmarking the reattachment lengths obtained from the developed numerical code against those reported in extant literature. The comparative analysis reveals a high degree of concordance between the present numerical predictions and previously established results, thereby substantiating the accuracy and robustness of the implemented algorithm. Principal outcomes and salient conclusions of the study are delineated in the ensuing sections.

- The computed reattachment points in the present analysis is in strong agreement with the values present in the literature.
- It is observed that when micromagnetorotation is taken into account, the reattachment point is lower than when it is not.
- Due to the magnetization effect, the flow is experiencing resistance in flow speed when the MMR effect is present, which causes the reattachment length to decrease.
- The reduction in reattachment length when the magnetization MMR effect is taken into account is more pronounced when the Reynolds number is lower than when it is greater.
- It is observed noted that as the Reynolds number rises, so does the stream function's maximum value.
- When the MMR impact is taken into account, the stream function's maximum value is lower than that of the stream function's maximum value which is obtained without MMR impact. This is because of the action of magnetization, which lowers stream function height by reducing flow speed.

In future, the present analysis can be extended to study the flows in more complex channel flows. Moreover, the model can also be extended to three-dimensional setting where more realistic geometrical consideration can be taken for related industrial applications.

Bibliography

- [1] J. Rajasekaran. *On the flow characteristics behind a backward-facing step and the design of a new axisymmetric model for their study*. University of Toronto, ON, Canada, 2011.
- [2] L. Chen, K. Asai, T. Nonomura, G. Xi, and T. Liu. A review of backward-facing step BFS flow mechanisms, heat transfer and control. *Thermal Science and Engineering Progress*, 6:194–216, 2018.
- [3] A.A. Al-Aswadi, H.A. Mohammed, N.H Shuaib, and Antonio Campo. Laminar forced convection flow over a backward facing step using nanofluids. *International Communications in Heat and Mass Transfer*, 37(8):950–957, 2010.
- [4] H. Iwai, K. Nakabe, and K. Suzuki. Flow and heat transfer characteristics of backward-facing step laminar flow in a rectangular duct. *International Journal of Heat and Mass Transfer*, 43(3):457–471, 2000.
- [5] J.H. Nie and B.F Armaly. Convection in laminar three dimensional separated flow. *International Journal of Heat and Mass Transfer*, 47(25):5407–5416, 2004.
- [6] B.F. Armaly, F. Durst, J.C.F Pereira, and B. Schönung. Experimental and theoretical investigation of backward-facing step flow. *Journal of Fluid Mechanics*, 127:473–496, 1983.
- [7] F. Selimefendigil and H. F. Öztöp. Numerical investigation and reduced order model of mixed convection at a backward facing step with a rotating cylinder subjected to nanofluid. *Computers & Fluids*, 109:27–37, 2015.

- [8] E. Abu-Nada. Application of nanofluids for heat transfer enhancement of separated flows encountered in a backward facing step. *International Journal of Heat and Fluid Flow*, 29(1):242–249, 2008.
- [9] J.G. Saldana, N.K Anand, and V. Sarin. Numerical simulation of mixed convective flow over a three-dimensional horizontal backward facing step. *Journal of Heat Transfer*, 127(9):1027–1036, 2005.
- [10] H.I. Abu-Mulaweh. A review of research on laminar mixed convection flow over backward and forward-facing steps. *International Journal of Thermal Sciences*, 42(9):897–909, 2003.
- [11] F. Selimefendigil and H.F. Öztop. Identification of forced convection in pulsating flow at a backward facing step with a stationary cylinder subjected to nanofluid. *International Communications in Heat and Mass Transfer*, 45:111–121, 2013.
- [12] A. Kumar and A.K. Dhiman. Effect of a circular cylinder on separated forced convection at a backward-facing step. *International Journal of Thermal Sciences*, 52:176–185, 2012.
- [13] A. S. Kherbeet, H.A. Mohammed, and B.H. Salman. The effect of nanofluids flow on mixed convection heat transfer over microscale backward-facing step. *International Journal of Heat and Mass Transfer*, 55(21-22):5870–5881, 2012.
- [14] A. S. Kherbeet, H.A. Mohammed, B.H. Salman, H. E. Ahmed, O. A. Alawi, and M. Rashidi. Experimental study of nanofluid flow and heat transfer over microscale backward-and forward-facing steps. *Experimental Thermal and Fluid Science*, 65:13–21, 2015.
- [15] F. Selimefendigil and H.F. Oztop. Control of laminar pulsating flow and heat transfer in backward-facing step by using a square obstacle. *Journal of Heat Transfer*, 136(8):081701, 2014.
- [16] F. Selimefendigil and H.F. Öztop. Laminar convective nanofluid flow over a backward-facing step with an elastic bottom wall. *Journal of Thermal Science and Engineering Applications*, 10(4):041003, 2018.

- [17] E. M.P. Cosserat and F. Cosserat. *Théorie des corps déformables*. A. Hermann et fils, 1909.
- [18] A.C. Eringen. Theory of micropolar fluids. *Journal of mathematics and Mechanics*, pages 1–18, 1966.
- [19] M.S. Khan and K. Hackl. Modeling of microstructures in a cosserat continuum using relaxed energies: Analytical and numerical aspects. In *Variational Views in Mechanics*, pages 57–87. Springer, 2021.
- [20] S. Sharma, S. Lambha, V. Mittal, and R. Verma. Micropolar lubricant effects on the performance of partial journal bearings. *Proceedings of the Institution of Mechanical Engineers, Part J: Journal of Engineering Tribology*, 237(7): 1461–1470, 2023.
- [21] M. S. Khan and K. Hackl. Modeling of microstructures in a cosserat continuum using relaxed energies. *Trends in Applications of Mathematics to Mechanics*, pages 103–125, 2018.
- [22] E. Karvelas, G. Sofiadis, T. Papathanasiou, and I. Sarris. Effect of micropolar fluid properties on the blood flow in a human carotid model. *Fluids*, 5(3):125, 2020.
- [23] N. S. Khan, T. Gul, S. Islam, and W. Khan. Thermophoresis and thermal radiation with heat and mass transfer in a magnetohydrodynamic thin-film second-grade fluid of variable properties past a stretching sheet. *The European Physical Journal Plus*, 132:1–20, 2017.
- [24] P.V. S. Narayana, B. Venkateswarlu, and S. Venkataramana. Effects of hall current and radiation absorption on mhd micropolar fluid in a rotating system. *Ain Shams Engineering Journal*, 4(4):843–854, 2013.
- [25] M.S. Khan and I. Hameed. A new magneto-micropolar boundary layer model for liquid flows—effect of micromagnetorotation (mmr). *arXiv preprint arXiv:2308.08457*, 2023.

-
- [26] A.J. Chamkha and F. Selimefendigil. Forced convection of pulsating nanofluid flow over a backward facing step with various particle shapes. *Energies*, 11 (11):3068, 2018.
- [27] R.K. Rajput. *A textbook of fluid mechanics and hydraulic machines*. S. Chand Publishing, 2004.
- [28] J.N. Reddy and D.K. Gartling. *The finite element method in heat transfer and fluid dynamics*. CRC press, 2010.
- [29] C.P. Kothandaraman. *Fundamentals of heat and mass transfer*. New Age International, 2006.
- [30] W.M. Rohsenow, J.P. Hartnett, Y.I. Cho, et al. *Handbook of heat transfer*, volume 3. Mcgraw-hill New York, 1998.
- [31] J. Kuneš. Thermomechanics. *Dimensionless Physical Quantities in Science and Engineering*. Elsevier, Oxford, pages 173–283, 2012.
- [32] M. KenThomasset and F. Jacques. Analysis of a laminar flow over a backward facing step. *Notes on numerical fluid mechancis*, 9:001–420, 1984.